RESEARCH ARTICLE

European Journal of Soil Science **WILEY**

Organic carbon enables the biotic engineering of beneficial soil structure in Profundihumic and Haplic Ferralsols

Pedro Martinez[1,2] | Rebecca A. Lybrand[3] | Karis J. McFarlane[4] | Maoz Dor[5] | Adrian C. Gallo[1] | Amy Mayedo[1] | Fillipe Marini[6] | Pablo Vidal-Torrado[7] | Markus Kleber[1]

[1]Department of Crop and Soil Science, Oregon State University, Corvallis, Oregon, USA

[2]New Mexico State University, Las Cruces, New Mexico, USA

[3]Department of Land, Air, and Water Resources, University of California-Davis, Davis, California, USA

[4]Lawrence Livermore National Laboratory, Center for Accelerator Mass Spectrometry, Livermore, California, USA

[5]School of Chemical, Biological, and Environmental Engineering, Oregon State University, Corvallis, Oregon, USA

[6]Department of Geosciences, Agroecology Graduate Program, Federal University of Paraíba, João Pessoa, Brazil

[7]Department of Soil Science, "Luiz de Queiroz" Agriculture College, University of São Paulo, Piracicaba, Brazil

Correspondence
Pedro Martinez, Department of Crop and Soil Science, Oregon State University, Corvallis, OR, USA.
Email: pedro.martinez@oregonstate.edu

Abstract

We investigated how organic matter may, directly and indirectly, modify the porosity of Ferralsols, that is, deeply weathered soils of the tropics and subtropics. Although empirical and anecdotal evidence suggests that organic matter accumulation may increase porosity, a mechanistic understanding of the processes underlying this beneficial effect is lacking, especially so for Ferralsols. To achieve our end, we leveraged the fact that the Profundihumic qualifier of Ferralsols (PF) is distinguished from Haplic Ferralsols (HF) by both a much larger average carbon content in the first 1 m of soil depth (19 kg C m^{-3} in PF vs. 10 kg C m^{-3} in HF) and a significantly lower bulk density (1.05 $\pm$ 0.08 kg L^{-1} in PF vs. 1.21 $\pm$ 0.05 kg L^{-1} in HF). Through exhaustive modelling of carbon – bulk density relationships, we demonstrate that the lower bulk density of PF cannot be satisfactorily explained by a simple dilution effect. Rather, we found that bulk density correlated with carbon content when combined with carbon: nitrogen ratio ($r^2 = 0.51$), black carbon content ($r^2 = 0.75$), and Δ^{14}C ($r^2 = 0.81$). Total pore space was greater in PF (61 $\pm$ 3%) than in HF (55 $\pm$ 2%), but x-ray computed tomography revealed that pore space inside soil aggregates of 4–5 mm diameter does not vary between the studied Ferralsols. We further observed nearly twice as many roots and burrows in PF compared with HF. We thus infer that the mechanism responsible for the increase in porosity is most likely an enhancement of resource availability (e.g., energy, carbon, and nutrients) for the organisms (earthworms, ants, termites, etc.) that physically displace soil particles and promote soil aggregation. As a result of increased resource availability, soil organisms can create especially the meso-scale structural soil features necessary for unrestricted water flow and rapid gas exchange. This insight paves the way for the development of land management technologies to optimize the physical shape and capacity of the soil bioreactor.

KEYWORDS
bulk density, Oxisols, radiocarbon, roots, soil fauna, X-ray tomography

1 | INTRODUCTION

Soil organic matter contributes to a wide range of crucial ecosystem services, including habitats for organisms, water purification and storage, carbon reservoir, and production of food, fibre, and fuel (Hoffland et al., 2020; Schmidt et al., 2011). The capacity of soils to store water and carbon is constrained by the total pore space (Vogel et al., 2022). But there are still uncertainties about the mechanisms that lead to changes in total soil pore space in response to organic matter contents (Regelink et al., 2015). Here, we investigate how the accumulation of organic matter may, directly and indirectly, modify the porosity and related bulk density of Ferralsols, which are deeply weathered soils occupying nearly 750 million hectares worldwide with a unique microaggregate ($\leq$3 mm diameter) architecture and comparatively large pore space (Buol & Eswaran, 1999; Neufeldt et al., 1999). We leverage natural examples of high carbon stocks in Profundihumic Ferralsols (19 kg C m^3) compared with other Ferralsols (10 kg C m^3, Batjes, 1996) to address the following research question: Is there *a causal relationship between organic matter content and porosity in Profundihumic Ferralsols?*

To address this question, we acknowledge that Profundihumic Ferralsols receive carbon inputs via two mechanisms: (1) allocation of carbon to belowground plant components that were transported by soil fauna (termites and ants) from aboveground to belowground; and/or (2) geomorphic deposition of eroded soil materials bearing organic matter (Martinez et al., 2022). Both mechanisms have implications for total soil pore space. The growth of extensive plant roots (mechanism1) can displace soil materials but also compact the vicinity of roots and reduce local soil porosity (Bruand et al., 1996; Xiong et al., 2022). To increase the total porosity in a volume of soil, part of the soil material needs to be transported to the surface or out of the soil which can be done by soil fauna, for example, earthworms, ants, and termites (Johnson et al., 2005; Swanson et al., 2019). An erosion-deposition process (mechanism2) may imply that soil constituents are remixed during downhill transport and may settle as a less dense material than before erosion.

Other factors potentially influencing soil porosity and bulk density are mineralogical composition; particle-size distribution (i.e. the percentage of sand, silt, and clay); frequency of wetting-drying cycles; organic matter content; and intensity of bioturbation, that is, the physical displacement of soil materials by organisms (Regelink et al., 2015; Ruehlmann & Körschens, 2009; Wilkinson et al., 2009). The influence of these factors on soil porosity and bulk density differs between soil types. Among

> **Highlights**
> - A model is provided on how organic matter accumulation increases the porosity of Ferralsols.
> - Low bulk density of carbon-rich Ferralsols is not caused by a simple particle dilution effect.
> - Organic matter increases the porosity of Ferralsols by stimulating natural bioturbation processes.

soils with variable charge (e.g., Ferralsols, Andosols, and Podzols), the low bulk density of Andosols (<1.0 kg L^{-1}) is caused by the high microporosity of clay minerals composed of hollow sphere allophane and fibrous imogolite with a high specific surface area of 300–600 m^2 formed through the rapid weathering of the glassy and volcanic ashes materials (Kleber & Jahn, 2007). Such minerals may also be found in podzol-Bs horizons which can be responsible for the low bulk density of some Podzols (Farmer, 1982). In the case of Ferralsols, their rather low bulk density (0.87–1.18 g cm^{-3}, $n = 80$, Volland-Tuduri et al., 2005) is largely attributed to a high porosity within and between microaggregates with "pseudo-sand" structure that is physically stable against dispersion (Martinez & Souza, 2020; Schaefer, 2001).

The microaggregation in Ferralsols is driven by geochemical and biological processes (Bruand et al., 2022; Buol & Eswaran, 1999; Schaefer, 2001). Geochemical transformation in Ferralsols occurs under intense and extended weathering that results in a clay mineral fraction dominated by low activity 1:1 phyllosilicates (kaolinite) and pedogenic Fe- and/or Al-(hydr)oxides, for example, haematite, goethite, and gibbsite (Schaefer et al., 2008). A recent study revealed that total pore space in Oxisols (Ferralsols counterpart in Soil Taxonomy) increases as the gibbsite/kaolinite ratio increases and the haematite/(haematite+goethite) ratio decreases (Pessoa et al., 2022). Pessoa et al. (2022) showed that Rhodic Haplustox (Rhodic Ferralsols) have the highest total pore space among Oxisols equivalent to Xanthic, Geric, and Haplic Ferralsols. Therefore, if the clay mineralogy of Profundihumic Ferralsols were the reason for a greater porosity of PF compared to other Ferralsols, we should observe (i) a higher gibbsite/kaolinite ratio and a lower haematite/(haematite+goethite) than in Rhodic Ferralsols (Pessoa et al., 2022); and (ii) little variation in mineralogical composition among Profundihumic Ferralsols. However, the clay mineralogy of Profundihumic Ferralsols varies substantially according to the parent material (Marques et al., 2011; Schaefer et al., 2008).
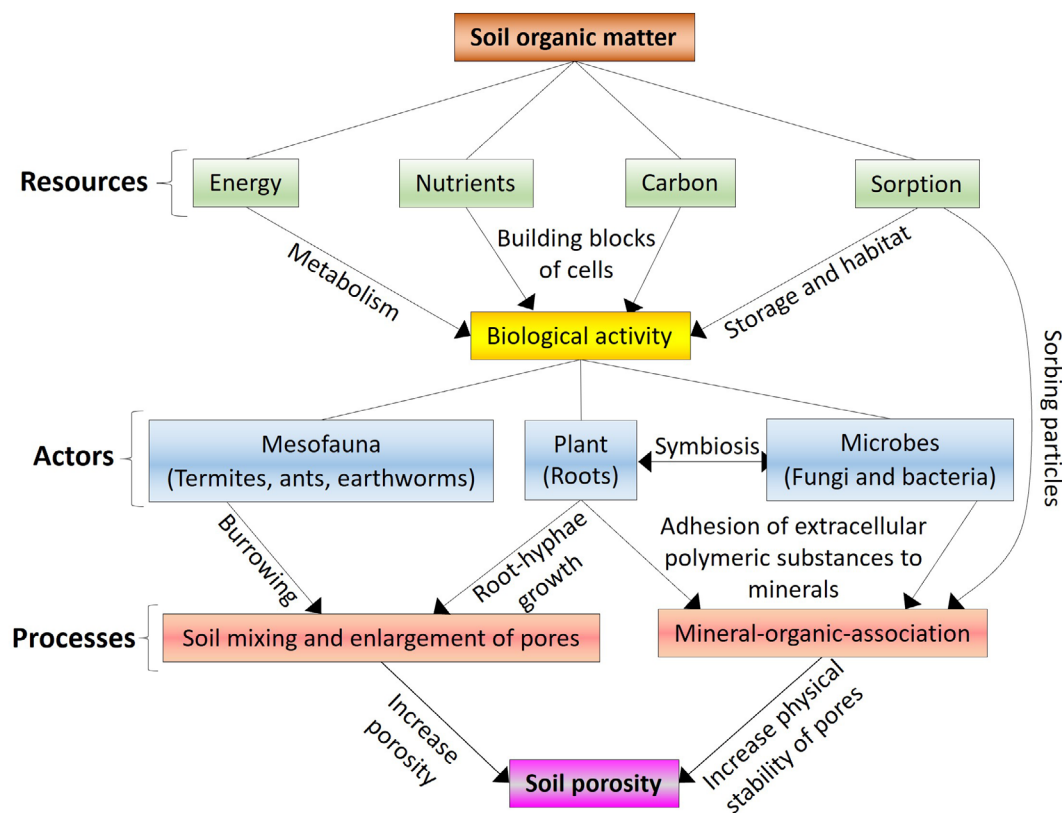
FIGURE 1 Conceptual model of the indirect effects of organic matter on soil porosity and bulk density. High additions of organic matter in Profundihumic Ferralsols may enhance the resources (energy, nutrient, carbon, and sorption) for bioturbation actors, such as plants, soil macrofauna (termites, ants, and earthworms), and microbes (fungi and bacteria). By stimulating biological activity (e.g., root growth and animal burrowing), organic matter can indirectly increase soil porosity and decrease bulk density.

Profundihumic Ferralsols formed from siliciclastic rocks in northeastern and southeastern Brazil have essentially kaolinitic clay mineralogy and little oxide content ($Fe_2O_3 = 32$ g kg^{-1} and $Al_2O_3 = 149$ g kg^{-1}), whereas Profundihumic Ferralsols formed from basalt in southern Brazil have significantly greater oxide contents ($Fe_2O_3 = 150$ g kg^{-1} and $Al_2O_3 = 291$ g kg^{-1}) and lower kaolinite content than other Ferralsols (Araujo et al., 2017; Calegari, 2008). Therefore, we can eliminate mineralogical composition as the main predictor for differences in bulk density (and porosity) between Profundihumic Ferralsols and other Ferralsols.

Aside from mineralogical composition, it is well-known that particle-size distribution (% of sand, silt, and clay) is a deterministic factor for soil porosity and related bulk density (De Vos et al., 2005; Tranter et al., 2007). To test particle size distribution as a predictor for bulk density, we hypothesized that bulk density in Profundihumic Ferralsols is a function of (i) clay content, (ii) clay + silt content, and (iii) sand content.

Soil bulk density may also be directly reduced by adding large quantities of soil organic matter because the average density of organic matter ($\sim$1.3 kg L^{-1}; Adams, 1973) is less than that of soil minerals ($\sim$2.7 kg L^{-1}; Curtis & Post, 1964). Hence, we hypothesized that organic matter modifies *bulk density through simple dilution of mineral particle density*.

Addition of organic matter with a certain composition (e.g., carbon: nitrogen (C/N) ratio and pyrogenic carbon content) may enhance the resource availability (energy, nutrient, and carbon) for plants, macrofauna (termites, ants, and earthworms), and microbes (fungi and bacteria) (Figure 1) (Hoffland et al., 2020; Lehmann et al., 2011; Zhang et al., 2020). Organic matter composition may thus indirectly influence bulk density and soil porosity by constraining the activity of bioturbation actors (soil biota) responsible for the physical displacement of soil materials through root growth and animal burrowing (Figure 1). Quantification of C/N ratios, pyrogenic carbon contents, and natural $^{13}C/^{12}C$ isotope ratios ($\delta^{13}C$) uniquely record information relating to sources of soil organic matter and its constituent parts (Amelung et al., 2008). To assess organic matter impacts on bioturbation actors that influence soil porosity, we hypothesized that *the bulk density of Profundihumic Ferralsols is a function of carbon: nitrogen (C/N) ratio, black carbon (BC) content, and carbon isotope concentrations*. Considering that bioturbation
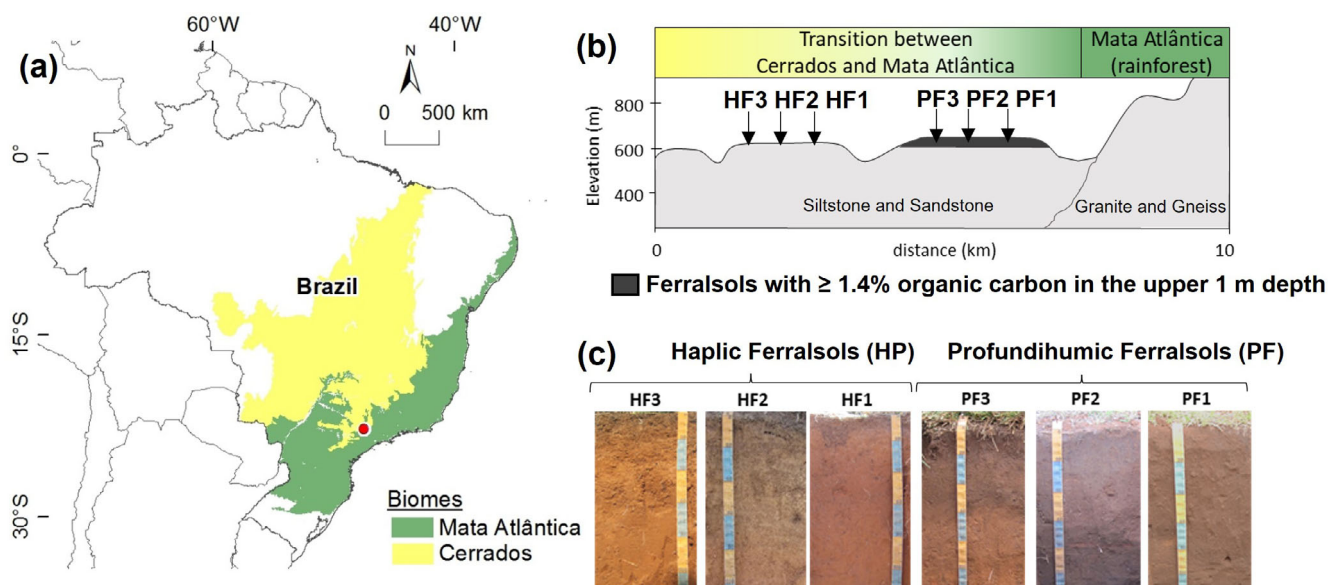
FIGURE 2 (a): Study area in southeastern Brazil. (b): Schematic topographic cross-section with the indication of the biomes and investigated soil profiles on correlated geomorphic surfaces and geological settings. (c): Photos of the studied Ferralsol profiles.

intensity may modulate soil porosity (Capowiez et al., 2021; Swanson et al., 2019), we hypothesized that *bulk density is inversely correlated with the abundance of morphological evidence for bioturbation (more burrowing and rooting = lesser bulk density)*.

Our conceptual approach is based on the recognition that Profundihumic Ferralsols consistently have lower bulk density than other Ferralsols (Martinez et al., 2022). Leveraging the fact that Haplic Ferralsols have the base levels of organic carbon content and bulk density, we initially determined the magnitude of an increase in organic matter content in Haplic Ferralsols that would be sufficient to reduce their bulk density to the same levels as seen in Profundihumic Ferralsols. To identify alternative, biologically mediated pathways towards an increase in porosity in Ferralsols, we conducted a comparative examination of soil morphology (e.g., roots and burrows contents), particle size distribution, porosity, water-stable aggregates, C/N ratio, BC content, and carbon isotope concentrations. Our comparison between Profundihumic Ferralsols versus Haplic Ferralsols encompasses the first 100 cm of soil depth to elucidate the direct and indirect effects of organic matter content on bulk density in the surface and subsurface soils.

2 | MATERIALS AND METHODS

2.1 | Study area

The Ferralsols investigated for this study are distributed in two sites located on correlated geomorphic surfaces at an elevation of 640 m above sea level and latitude/ longitude of 23°00′40″S/47°09′01″W and 23°01′22″S 47°09′09″W in Campinas, São Paulo state, southeastern Brazil (Figure 2). The soils are derived from siltstone and fine sandstone of the Itararé Group (Palaeozoic) and Rio Claro Formation (Cenozoic) (IPT, 1981). The Ferralsols considered here are on flat geomorphic surfaces characterized as pediplains, that is, extensive plains formed by the coalescence of pediments that are stable in terms of erosion processes and without evidence of colluvium deposition (Ross & Moroz, 1996). These geomorphic surfaces were preserved as remnants from the planation processes of the landscape that occurred at the end of the Pliocene and during the Pleistocene (Villela et al., 2013). The present land use of the areas of all studied soil profiles is regenerated vegetation composed of grasses and arboreal elements of semi-deciduous forests with mixed characteristics of the Cerrados (savanna) and Mata Atlântica (rainforest) biomes (Calegari, 2008). The remaining native vegetation in the Municipality of Campinas is made up of rainforests and savanna (Santin, 1999). The resulting diversity of species underlines the ecological importance of this area (Ferreira et al., 2007). Pollen records in the soils of the study area indicate drier conditions in the early Holocene (∼10 thousand years ago) that induced the development of the open-field vegetation of Cerrados with fire incidence while the installation of a humid climate between 3 to 2 thousand years ago led to an expansion of the rainforest (Aviles et al., 2019). The land use history of this area is similar to other areas in the vicinity of Campinas. These areas likely underwent

suppression of primary vegetation when converted to agricultural use (coffee, sugar cane, and pasture). Such land use changes started in the XIX century with the expansion of colonization towards the west of São Paulo state. The area likely was used for agricultural or grazing production, but specific information about local land use history is limited. Although we do not have the precise year of vegetation suppression, we are confident that the sites remained under similar land use since 1950 when they were annexed to the airport's security zone. The climate in this region is Humid Subtropical (Cfa in Köppen's Classification System), with a mean annual precipitation of 1344 mm and a mean annual temperature of 21°C (Alvares et al., 2013).

2.2 | Soil morphology, sampling, and basic analysis

A total of six soil profiles were described and sampled (Figure 2). Three soil profiles are Profundihumic Ferralsols identified as PF1, PF2, and PF3, which are nearly 1.3 km apart from the three Haplic Ferralsol profiles designated as HF1, HF2, and HF3 (Figure 2). Soil profiles were investigated in excavated pits with the following morphological attributes described in the field according to Schoeneberger et al. (2012): horizon designation, colour, structure types, texture, and the quantity and size of roots and pores. Soils were sampled by depth increment: 0–20, 20–40, 40–60, and 60–100 cm, to compare soil properties between Ferralsols at the same soil depth intervals. Our point of using the upper 100 cm soil depth to compare Profundihumic versus Haplic Ferralsols is to show the direct and indirect effects of organic matter content on soil porosity across different soil depths.

Soil samples were air-dried, sieved (2 mm), and prepared for particle size and chemical analysis described as follow. To disperse elementary particles before clay content determination, 40 g of air-dried soil was dispersed with 16 h shaking treatment in 250 mL solution composed of NaOH (0.1 mol L^{-1}) and $(NaPO3)_6$ (0.015 mol L^{-1}). Clay content was estimated using the hydrometer method, while the sand content was quantified after sand separation using wet sieving. Determination of basic soil properties included soil pH in water and KCl, cation exchange capacity (CEC) determined with 1 M NH_4OAc at pH 7, total carbon and nitrogen content measured with a LECO elemental analyser, water-stable aggregates (% of total soil mass) estimated with simulated rainfall (Gugino et al., 2009), and soil bulk density.

To determine the bulk density (Db) of each depth interval, we collected triplicate undisturbed soil cores using stainless steel cylinders with a diameter of 3.6 cm

and a height of 5.4 cm. Bulk density was estimated as the weight of oven-dried (105°C) soil divided by core volume. We calculated total porosity (φ) based on bulk density (Db) and particle density (Dp = 2.65 kg L^{-1}, average particle density of Ferralsols from the study area, Calegari, 2008) according to Equation 1.

$$\varphi(\%) = 100 - \left(\frac{\text{Db soil}}{\text{Dp}} \times 100 \right) \quad (1)$$

Total carbon (C) and nitrogen (N) for each soil depth interval are given as concentration of mass of C or N per mass of dry soil (g kg $soil^{-1}$) according to Equation 2. The mass of the soil dried at 105°C is the mass reference.

$$\text{C or N} = \frac{\text{C or N mass}}{\text{Dry soil mass}} \quad (2)$$

For soil classification purposes and stock estimations, we calculated carbon and nitrogen concentrations for the entire first 1 m of depth as a weighted average (C% and N% w.t.) according to Equation 3, where t is the thickness (cm) of the depth intervals.

$$\text{C or N}(0-100 \text{ cm soil depth}) = \frac{\sum (t \times C\% \text{ or N\%})}{100} \quad (3)$$

The stocks of C and N in the upper 1 m (10 dm) of soil profile depth were estimated according to Equation 4, where RF is rock fragment content (% of the total mass of soil) measured by weighing the total rock fragments retained on a 2 mm sieve:

$$\text{C or N}\left(\text{kg m}^{-3}\right) = \text{C or N } (\%\text{w.t.}) \times 10 \text{ dm} \times \text{Db}\left(\text{kg L}^{-1}\right) \\ \times \frac{100 - \%\text{RF}}{100} \quad (4)$$

Morphological, physical, and chemical soil properties were used to test our hypotheses and to classify the soil profiles according to the World Reference Base for Soil Resources (IUSS Working Group WRB, 2022).

2.3 | Carbon fractionation with NaOCl

We employed a carbon fractionation technique to determine carbon content and isotopic characteristics (δ^{13}C and Δ^{14}C) of mineral-associated and total soil organic matter. This allowed us to determine whether bulk density is dependent on the ratio between mineral-associated and overall (total) carbon. Sodium hypochlorite (NaOCl) was used to oxidize and remove carbon from soil organic

matter that is unprotected by mineral phases (Siregar et al., 2005). The residue after NaOCl oxidation was considered mineral-protected carbon (Kleber et al., 2005). The experimental procedure of the NaOCl treatment is described as follow. Briefly, 10 g of air-dried soil was reacted with 100 mL of a solution of 6% NaOCl adjusted to pH 8.0 by adding 32% HCl. Three treatment cycles of 6 h each were conducted at 25°C. Samples were centrifuged (2574 × g; 5 min), decanted, and the residues washed twice using 100 mL 1 M NaCl and shaken overnight with deionized water. Excess salts were removed by dialysis using a membrane of 12–14,000 Da. When the electrical conductivity reached <40 μs cm^{-1}, the samples were freeze-dried for further measurements of total carbon and nitrogen contents and isotopic analysis (δ^{13}C and Δ^{14}C).

2.4 | Carbon isotope analysis

The concentrations of carbon isotopes (^{13}C and ^{14}C) in combination with other parameters (e.g., C/N ratio) were used to make inferences about the composition and turnover characteristics of the soil organic matter. We understand that Δ^{14}C values of soil organic matter do not represent exactly how long the material has been in the soil given that soil organic matter is continuously cycling and receiving new carbon inputs while part is being lost as CO_2 (Torn et al., 2009). However, the Δ^{14}C values obtained in our study were used to provide quantitative measures of the radiocarbon content that is considered modern (after the year 1950) when δ^{14}C values are positive versus negative Δ^{14}C values indicating pre-modern sample (Stuiver & Polach, 1977). In addition, the ^{14}C radiocarbon age of large charcoal fragments (≥ 1 cm diameter) was used to infer the fire history of the field area and to estimate burial rates of the soil surface by soil animals (ants, termites, and earthworms). It is well known that soil animals effectively transport soil materials to the ground surface and equally bring material from the surface to belowground (Johnson et al., 2005; Johnson & Schaetzl, 2015). This transport of soil materials results in the burial of large objects (e.g., charcoal fragments, cinders, flints, and archaeological artefacts) left on the ground surface (Darwin, 1881; Johnson et al., 2005). As a result, the known age of large charcoals left on the ground surface has been applied to quantify burial rates of the soil surface by bioturbation (Boulet et al., 1995).

The concentration of the stable carbon isotope ^{13}C is presented herein as δ^{13}C (see Equation 5), where δ^{13}C is a measure of the ratio ^{13}C:^{12}C in terms of isotope concentrations. The international standard USGS40

(glutamic acid 40) was used in the δ^{13}C calculation. Measured Δ^{13}C values were used to correct for mass-dependent fractionation in the Δ^{14}C notation in Equation 6, where A_{sn} is the normalized sample activity normalized for mass dependent isotopic fraction A_{on} is the is the standard specific activity of the standard (Oxilic Acid, primary ^{14}C isotopic standard) normalized for mass dependent isotopic fractionation, lambda is 1/8267 year^{-1}, and x is the year of measurement (2021) (Stuiver & Polach, 1977). The results of δ^{13}C and Δ^{14}C are expressed in the delta per mil notation (‰).

$$\delta^{13}C(\text{‰}) = \left(\frac{\frac{13_C}{12_C}\text{sample}}{\frac{13_C}{12_C}\text{standard}} - 1 \right) \times 1000 \tag{5}$$

$$\Delta^{14}C(\text{‰}) = \left(\frac{A_{sn}e^{\lambda(1950-x)}}{A_{ON}} - 1 \right) \times 1000 \tag{6}$$

δ^{13}C and Δ^{14}C were determined in bulk-untreated soils and in NaOCl-treated soils from all investigated soil depth intervals of profiles PF1, PF2, PF3, and HF1. Taking that NaOCl-treated soils contain more mineral-protected organic matter than bulk-untreated soils, we determine whether bulk density is dependent on the ratio between isotope concentrations of mineral-associated and overall (total) carbon. We also determined δ^{13}C and Δ^{14}C of charcoal fragments (≥ 1 cm diameter) found at 55 cm of soil depth in profile PF2. The concentration of the isotope ^{13}C in the soil samples was analysed with continuous-flow isotope ratio mass spectrometry using a Carlo Erba elemental analyser connected to a Thermo DeltaPlus isotope ratio mass spectrometer at the Stable Isotope Laboratory, Oregon State University (Corvallis, USA). Radiocarbon ^{14}C contents were measured by a NEC 1.0 MV Tandem accelerator mass spectrometer (AMS) at the Center for AMS at Lawrence Livermore National Laboratory (California, USA). Instrument and the sample preparation and graphitization process used for radiocarbon ^{14}C analysis are described in Broek et al. (2021). Following archaeological protocol, the conventional radiocarbon age of charcoal fragments was calculated with Equation 7 where $F = (N_0/N)$, N_0 = the number of atoms of the isotope in the original sample at time 0, and N the number of atoms left after time t which assumes the Libby half-life (5568 years; mean life 8033 years, mean life = the average time a given atom will survive before undergoing radioactive decay) rather than the correct value of 5730 years (Stuiver & Polach, 1977) and were referenced to 1950 as 1950 A.D. = 0 B.P.

$$^{14}\text{C age of charcoal fragments} = -8033 \text{ years } \ln F^{14}C$$
$$\tag{7}$$

2.5 | Black carbon determinations

Pyrogenic organic matter such as charcoal is produced by the incomplete combustion of organic matter. Charcoal is a highly porous and low-density material whose physical properties play a key role in total soil porosity (Batista et al., 2018). Because studies reported that Profundihumic Ferralsols have high charcoal contents (Marques et al., 2015; Velasco-Molina et al., 2016), we examined to what extent the pyrogenic organic matter content affects the total porosity of Profundihumic Ferralsols in comparison to Haplic Ferralsols. To this, black carbon content (i.e. thermally altered carbon particles having a graphitic microstructure) in all 26 soil samples were quantified using the benzene polycarboxylic acid (BPCA) method (Glaser et al., 1998). This method uses nitric acid to oxidize the extended condensed aromatic sheets (graphite structure) into individual carboxylated benzene rings that can be isolated and quantified using high performance liquid chromatography (HPLC). Soil samples containing ~5 mg of organic carbon were digested in 5 mL HNO_3 at 170°C for 8 h using pressurized microwave vessels (Mars 6, CEM). Samples were filtered through glass fibre filters (Whatman, GF/A) and the remaining solids were washed with 5 mL of NaOH (1 M). Samples were diluted to 50 mL with deionized water, frozen with liquid nitrogen, and freeze-dried (LabConco FreeZone Plus). A 1 mL aliquot of sample was transferred to a clean vial and analysed in a HPLC Shimadzu. External standards of pure BPCA solutions were used to construct 6-point calibration curves to determine the concentrations of individual BPCAs. The separation and quantifications of BPCAs (B3CA, B4CA, B5CA, and B6CA) were based on the area of the chromatography peak yielded by the HPLC. The sum of all BPCAs was used as an estimate of black carbon content as the percentage of total organic carbon.

2.6 | Soil porosity assessed with X-ray computed tomography

Total pore space and pore connectivity within soil aggregates of 4–5 mm diameter were estimated using x-ray computed tomography (Wildenschild & Sheppard, 2013). We deployed microtomography as opposed to large-scale tomography because the porosity of Ferralsols is not determined by macrostructure, rather, Ferralsol porosity is controlled by the arrangement of microaggregates (Balbino et al., 2002). The studied aggregates of 4–5 mm diameter in Ferralsols likely correspond to remnants structures (e.g., walls of galleries or cavities) created by earthworms (casts) or ants/termites burrowing activity and related material displacement within the whole soil

groundmass (Bruand & Reatto, 2022; Reatto et al., 2009). We separated soil aggregates using a sieve with manual agitation during 30 s and no force was applied to break large aggregates into small ones. We examined soil aggregates from 0 to 20 and 60 to 100 cm soil depth intervals from profiles PF1, PF2, HF1, and HF3. These depth intervals were chosen because we focused on the comparison between the surface and deep subsurface soils of Profundihumic Ferralsols and Haplic Ferralsols. For each soil depth interval, we examined 3 soil aggregates, amounting to a total of 24 soil aggregates. The images of the aggregates were acquired at Oregon State University's micro-CT facility. Scanning was performed in a helical trajectory at 80 kV tube voltage, 50 mA tube current with 0.5 s exposure time, and 0.8 mm aluminium filter. Helical cone-bean filtered back-projection was used for the reconstruction of 3D images and resulted in a voxel resolution of 3.5 μm. Image processing was performed in ImageJ software with a 3D median filter with a kernel size of 3 voxels ($3.5 \times 3.5 \times 3.5$ μm^3 in volume) followed by a 3D-shaped mask filter. To generate the binary images with particles in white and pore phases in black, the histogram of each set of soil aggregate images was joined, and the minimum grayscale value between the air and the soil matrix peaks was taken as the threshold value.

Pore space area analysis was achieved for the following pore types: (1) surface disconnected pores, that is, investigated pores without connection to the surface of the aggregate according to the equipment used. The pores were segmented by applying a 3D fill hole algorithm to fill all the internal isolated pores, and subtracting the filled image from the initial segmented image; and (2) surface connected pores defined by applying a black top-hat transform which defines the difference between a morphological closing algorithm and the segmented image. The volume of the soil aggregate was delineated using a morphological closure algorithm, and the space inside the aggregates was calculated as the volume fraction of the pore phase in the aggregated volume. Both pore types were merged into a single pore space to calculate the total pore space inside the studied soil aggregates. Using a watershed transform on the pore space image, the pore bodies were separated, and morphological metrics were calculated for each cluster to assess the different metric distributions. Pore connectivity was inferred according to the volume of disconnected pores. We calculated the Euler number for each soil aggregate to determine a topological invariant that serves as an indicator of connectivity defined according to Equation 8, where χ is the Euler number, $\beta 0$ is the number of clusters, $\beta 1$ is the number of redundant connections or loops, and $\beta 2$ is the number of cavities within the object. Negative Euler values

indicate a well-connected pore phase, while positive values indicate that the pore system is predominantly disconnected.

$$\chi = \beta 0 - \beta 1 + \beta 2 \qquad (8)$$

2.7 | Modelling the dilution of soil particle density

Previous studies have argued that organic matter directly reduces soil bulk density because the density of organic matter is less than that of soil minerals (Adams, 1973; Ruehlmann & Körschens, 2009). The underlying assumption here is that the bulk density of soils depends exclusively on the densities of phases that are present and on the relative contribution of each phase to the volume of interest. Using $1.3 \, kg \, L^{-1}$ as the presumed density of organic matter (P_{OM}) (Adams, 1973), we calculated the extent of organic matter accumulation required to achieve the observed difference in bulk density between Haplic and Profundihumic Ferralsols. Initially, bulk density for each depth interval of the studied Profundihumic Ferralsols and Haplic Ferralsol profiles was back-calculated according to the average density of solid constituents (organic matter and minerals). The volume of organic matter (V_{OM}) in the soil was calculated using its mass proportion and specific mass, that is, "particle density". The mass unit of oven-dried soil (M_{SOIL}, kg) is equal to the sum of a mass of mineral compounds (M_{MC}, kg) and a mass of organic matter (M_{OM}, kg) (Equation 9). And the bulk volume of the soil is equal (V_{SOIL}, $L \, kg^{-1}$) to the reciprocal of the bulk density (Db, $kg \, L^{-1}$). We estimated soil bulk density (Db') using equation 9, where P_{MC} ($2.685 \, kg \, L^{-1}$) and P_{OM} ($1.3 \, kg \, L^{-1}$) are the particle density of the mineral and organic matter compounds, respectively. We estimated M_{OM} using the conversion factor 2 of soil organic carbon (Pribyl, 2010). We adopted the reference value of $2.685 \, kg \, L^{-1}$ as P_{OM} since it is the average soil mineral density in the studied Profundihumic Ferralsols (Calegari, 2008).

$$M_{SOIL} = M_{MC} + M_{OM}$$

$$V_{SOIL} = 1/Db$$

$$V_{OM} = M_{OM}/P_{OM}$$

$$V_{MC} = M_{MC} + P_{MC}$$

$$Db' = \frac{1}{(V_{OM} + V_{MC})} = \frac{1}{\left(\frac{M_{MC}}{PM_{MC}} + \frac{M_{OM}}{P_{OM}}\right)} \qquad (9)$$

The estimated and measured soil bulk density are well correlated, $r^2 = 1.0$ (Data S1, Figure SI2.1a). Once

we validated our model, the concentration of organic matter was increased such that the bulk density of Haplic Ferralsols eventually reached the average bulk density of the studied Profundihumic Ferralsols (Data S2). We simulated the increase in organic matter content based on the starting value of carbon concentration that was measured in the studied soils.

2.8 | Data analysis

We used linear regressions with bulk density as the dependent variable whereas the following properties were treated as predictor variables: clay content, clay+silt content, pH, CEC, carbon concentration of untreated and NaOCl-treated soils, C/N ratio, black carbon content, and carbon isotope concentrations ($\delta^{13}C$ and $\Delta^{14}C$). The predictor variables with a moderate correlation with bulk density ($r^2 > 0.5$) were combined in multiple regression models and represented in 3D plots. For the multiple linear regressions, we normalized the data using z-score normalization. We used Student's t-test to determine statistical differences of the predictor variables between Profundihumic Ferralsols and Haplic Ferralsols for the whole control section (0–100 cm soil depth interval). We determine statistical differences for each soil depth interval (0–20, 20–40, 40–60, 60–100 cm) between Profundihumic Ferralsols and Haplic Ferralsols using ANOVA and Tukey's HSD test. All the statistical analyses were made in the software RStudio.

3 | RESULTS

3.1 | Soil morphology and classification

Profundihumic Ferralsols consistently displayed dark colours (value ≤3), a strong granular and a weak subangular blocky structure, and sandy clay texture to 1 m depth for all three soil profiles studied (Tables 1 and 2). Haplic Ferralsol profiles were lighter in colour (value ≥4) and presented evidence for structural and textural properties that were similar to the PF profiles, with the exception of profile HF3 which contained nearly 10% more clay than all the other profiles in the study (Tables 1 and 2). The absence of clay illuviation combined with low reactivity (CEC <9 $cmol_c \, kg^{-1}$) at subsurface (40–100 cm soil depth) is indicative of a ferralic diagnostic horizon (Tables 1 and 2). The Profundihumic Ferralsols studied here contain hyper-developed A-horizons that are at least 1 m thick. As a result, the entire vertical control section in the PF profiles of our study corresponds to the A horizon. This is evident when observing the dark

TABLE 1 Morphological attributes of the studied Profundihumic Ferralsols (PF) and Haplic Ferralsols (HF).

Soil profile/ soil class[a]	Depth cm	Hor[b]	Color[c] Moist	Struct[d]	Text[e]	Roots Quant[f]	Size[g]	Pores Quant[f]	Size[g]	Shape
PF1	0–20	A1	7.5YR 2.5/2	GR/SB	SC	M	M/F/VF	M	C/M/F	IR/DT/TU
	20–40	A2	7.5YR 3/2	SB/GR	SC	M	M/F	M	M/F	IR/DT/TU
	40–60	A3	7.5YR 3/3	SB/GR	SC	M	M/F/VF	C	M/F	IR/TU
	60–100	A3	7.5YR 3/3	SB/GR	SC	C	C/M/F	C	VC/M/F	IR/DT/TU
PF2	0–20	A1	7.5YR 2.5/2	GR/SB	SC	M	C/M/F	M	M/F	IR/DT/TU
	20–40	A2	7.5YR 3/3	SB/GR	SC	M	M/F	M	M/F	IR/TU
	40–60	A2	7.5YR 3/3	SB/GR	SC	M	M/F/VF	M	M/F	IR/TU
	60–100	A3	7.5YR 2.5/2	SB/GR	SC	C	C/M/F	C	C/M/F	IR/DT/TU
PF3	0–20	A1	5YR 3/2	GR/SB	SC	M	M/F/VF	M	M/F	IR/DT/TU
	20–40	A1	5YR 3/2	GR/SB	SC	M	M/F	M	M/F	IR/DT/TU
	40–60	A2	5YR 3/3	SB/GR	SC	M	C/M/F	C	C/M/F	IR/TU
	60–100	A3	5YR 4/3	SB	SC	C	M/F	C	MF	IR/DT/TU
HF1	0–20	A	5YR 4/3	GR/SB	SC	M	M/F/VF	M	C/M/F	IR/DT/TU
	20–40	AB	5YR 4/3	SB/GR	SC	M	M/F	M	M/F	IR/DT/TU
	40–60	B	5YR 5/4	SB/GR	SC	C	M/F	C	C/M/F	DT/TU
	60–100	B	5YR 5/4	SB	SC	F	F	C	MF	DT/TU
HF2	0–20	A	7.5YR 4/3	SB/GR	SC	M	M/F/VF	M	C/M/F	IR/DT/TU
	20–40	AB	7.5YR 4/4	SB/GR	SC	M	M/F	M	C/M/F	IR/TU
	40–60	B	7.5YR 5/4	SB	SC	F	F	C	M/F	IR/TU
	60–100	B	7.5YR 5/4	SB	SC	F	F	C	F	IR/DT
HF3	0–20	A	7.5YR 4/4	GR/SB	C	M	M/F/VF	M	C/M/F	IR/DT/TU
	20–40	AB	7.5YR 4/4	SB/GR	C	M	M/F	M	C/M/F	IR/DT/TU
	40–60	B	7.5YR 5/4	SB/GR	C	C	M/F	C	M/F	IR/TU
	60–100	B	7.5YR 5/4	SB	C	F	F	C	F	DT/TU

[a]Soil classification according to the World Reference Base for Soil Resources (IUSS Working Group WRB, 2022).

[b]Soil horizon designation.

[c]Munsell colour.

[d]Soil structure types: GR: granular, SB: subangular blocky. First code represents the dominant structure type.

[e]Soil texture class: SC: sandy clay; C: clay.

[f]Quantity as average count of roots and pores per assessed area of 10 cm^2: M: many ($\geq$ 5), C: common (1–5), F: few (<1).

[g]Size: C: coarse (5–10 mm diameter), M: medium (2–5 mm diameter), F: fine (1–2 mm diameter), VF: very fine (<1 mm diameter). Shape: IR: interstitial; DT: dendritic tubular; TU: tubular.

colour and abundance of roots along the first 1 m of soil depth (Table 1, Figure 2a). The dark colour (value ≤3) and high carbon concentration as a weighted average (C% w.t. ≥1.6, Table 2) in the first 1 m of soil depth in the PF profiles indicate the presence of an Umbric epipedon and satisfy the requirement for the Profundihumic qualifier (C% w.t. ≥ 1.4 and ≥1% soil organic carbon throughout) of the World Reference Base for Soil Resources (IUSS Working Group WRB, 2022). Therefore, profiles PF1, PF2, and PF3 are classified as Profundihumic Ferralsols. Because all soil profiles exhibited colours in the range of 5YR and 7.5YR, we excluded the qualifiers Xanthic and Rhodic. For the HF-profiles, the colour value ≥4 and the texture sandy clay or finer indicate the presence of an Ochric epipedon. Hence, all HF profiles key out as Haplic Ferralsols.

The visual assessment of soil profiles in the field (2D view) indicates that the subsurface (60–100 cm) of the studied Profundihumic Ferralsols contain 7 ± 2 roots per 10 cm^2, whereas Haplic Ferrasols have 2 ± 1 roots per 10 cm^2 (Figure 3, Table 1). For the entire control section (0–100 cm soil depth interval), Profundihumic Ferralsols contain twice as many roots as the Haplic Ferralsols (Figure 3). At the subsurface (60–100 cm soil depth), PF profiles have coarse and medium size roots (10–2 mm diameter) whereas Haplic Ferralsols contain predominantly fine size roots (<2 mm diameter). Some of these deep coarse roots in Profundihumic Ferralsols were dead and highly decomposed. Our visual assessment indicates that after the roots have been completely decomposed, they leave behind coarse and very coarse pores (Figure 3). The abundance of roots (≥5 roots per 10cm^2) in the subsurface (60–100 cm soil depth) strongly suggests the involvement of roots in the genesis of pores both at surface and subsurface soils.

There is a clear relationship between root and pore size in the subsurface soils. The average count of coarse roots and pores (5–10 mm diameter) is ≥5 per 10 cm^2 at 60–100 cm depth interval in Profundhumic Ferralsols, whereas Haplic Ferralsols have few (≤1 per 10 cm^2) coarse roots and pores at the same subsurface (Table 1). In terms of pore morphology, we identified interstitial pore shape (i.e. voids between microaggregates of sand size ≤2 mm) in the upper 40 cm and between 60 and 100 cm of soil depth. The frequency of interstitial pore shape in subsurface (>40 cm depth) soil is greater in Profundihumic Ferralsols than the Haplic Ferralsols. In all studied soils, we found dendritic/tubular pores (i.e., cylindrical, elongated, and branching voids) which can be empty and occupied by roots, especially at surface soils (0–30 cm), but we identified coarse dendritic/tubular pores at 60–100 cm soil depth. Medium tubular pores observed in the studied soil profiles may also be formed by earthworm activity. All soils consistently display interstitial pores connected as a network of channels which are likely related to ant or termite activity.

3.2 | Carbon and nitrogen contents

Average carbon stock and concentration from 0 to 100 cm soil depth are significantly higher in Profundihumic Ferralsols (18 ± 1 kg C m^{-2} and $1.7 \pm 0.1\%$ w.t.) than in Haplic Ferralsols (11 ± 2 kg C m^{-2} and $1.0 \pm 0.1\%$ w.t.), p-value = 0.01 (Table 2). The difference in carbon concentration between Profundihumic and Haplic Ferralsols increases substantially with soil depth (Figure 4b). In the first 20 cm of soil depth, Profundihumic Ferralsols contain a slightly higher carbon concentration (23 ± 3 g C kg^{-1}) than Haplic Ferralsols (17 ± 3 g C kg^{-1}). At 60 to 100 cm of soil depth, Profundihumic Ferralsols have more than double the carbon concentration (15 ± 2 g C kg^{-1}) of Haplic Ferralsols (6 ± 1 g C kg^{-1}), p-value = 0.01 (Figure 4b, Table 3). A similar pattern was observed for nitrogen content. Only at 60–100 cm of soil depth do Profundihumic Ferralsols show significantly greater nitrogen concentration (0.73 ± 0.12 g N kg^{-1}) than Haplic Ferralsols (0.45 ± 0.09 g N kg^{-1}), p-value = 0.06. Based on the depth-profile distribution of carbon and nitrogen contents, we infer that the effects of organic matter on the variability of bulk density between Profundihumic and Haplic Ferralsols are likely more relevant at the subsurface (60–100 cm soil depth) than near the soil surface.

The C/N ratios were significantly higher in Profundihumic Ferralsols (18 ± 2) than in Haplic Ferralsols (14 ± 1), p-value<0.001 (Figure 4c, Table 3). The C/N ratio follows the same depth profile distribution of BC content and Δ^{14}C (Figure 4c–e). In addition, the C/N ratio of the soils increased as a function of BC content in all soil depth intervals separately ($r^2 \geq 0.34$) and in the entire 0–100 cm soil depth ($r^2 = 0.59$) (Data S3, Figure SI3.5). Carbon concentration in NaOCl-treated soils is also greater in Profundihumic Ferralsols (8 ± 1 g C kg^{-1}) than in Haplic Ferralsols (5 ± 1 g C kg^{-1}), p-value< 0.01 (Figure 4f, Table 3).

3.3 | Black carbon content and charcoal occurrence

Profundihumic Ferralsols have greater BC content ($7 \pm 2\%$ of total C) than Haplic Ferralsols ($4 \pm 1\%$ of total C) in the first 100 cm of soil depth, p-value = 0.001. The difference in BC content between Profundihumic Ferralsols and Haplic Ferralsol also increases with soil depth

TABLE 2 Basic soil properties of the studied Profundihumic Ferralsols (PF) and Haplic Ferralsols (HF).

Soil profile/ soil class[a]	Depth cm	Bulk density Kg L^{-1}	Rock content[b] %	Pore space[c]	Sand	Silt	Clay	Water stable aggregate	pH H$_2$O	KCl	CEC[d] cmol$_c$ kg^{-1}	C[e] % w.t.	Kg m^{-2}	N[f] % w.t.[d]	Kg m^{-2}
PF1	0–20	1.10 ± 0.08	1.0 ± 0.2	58	50	5	45	86	4.5	4.1	8.5	1.91	19.4	0.11	1.07
	20–40	1.08 ± 0.05	0.5 ± 0.1	59	52	5	43	86	4.7	4.2	8.2				
	40–60	1.05 ± 0.04	0.3 ± 0.2	60	48	8	44	84	4.7	4.3	7.9				
	60–100	0.90 ± 0.02	0.7 ± 0.3	66	49	6	45	76	4.9	4.3	6.4				
PF2	0–20	1.12 ± 0.07	0.9 ± 0.3	58	52	6	42	85	5.1	4.2	8.3	1.61	16.1	0.09	0.92
	20–40	1.05 ± 0.04	0.4 ± 0.2	60	54	7	39	85	4.9	4.1	7.2				
	40–60	0.90 ± 0.05	0.2 ± 0.1	66	54	6	40	75	4.9	4.3	7.1				
	60–100	0.95 ± 0.05	0.4 ± 0.1	64	52	7	41	69	5.4	4.5	6.8				
PF3	0–20	1.14 ± 0.06	1.1 ± 0.3	57	55	10	35	83	4.9	4.1	7.5	1.67	18.2	0.10	1.09
	20–40	1.08 ± 0.07	0.6 ± 0.1	59	57	8	35	79	4.7	4.2	6.3				
	40–60	1.09 ± 0.04	0.6 ± 0.2	59	52	12	36	83	4.7	4.2	6.2				
	60–100	1.08 ± 0.04	0.8 ± 0.4	59	60	5	35	69	4.6	4.3	6.3				
HF1	0–20	1.26 ± 0.08	0.7 ± 0.2	52	49	12	39	77	4.9	4.1	6.9	1.19	13.8	0.09	1.03
	20–40	1.24 ± 0.07	0.3 ± 0.2	53	52	10	38	82	4.9	4.1	6.9				
	40–60	1.22 ± 0.05	0.5 ± 0.1	54	52	12	36	76	5.0	4.2	6.5				
	60–100	1.19 ± 0.05	0.4 ± 0.2	55	55	9	36	57	5.2	4.4	6.1				
HF2	0–20	1.29 ± 0.06	1.3 ± 0.5	51	49	4	47	74	4.7	4.2	6.5	0.86	10.3	0.06	0.67
	20–40	1.25 ± 0.03	0.8 ± 0.6	53	52	6	42	73	4.8	4.3	6.1				
	40–60	1.19 ± 0.05	0.7 ± 0.4	55	52	5	43	70	4.8	4.4	6.0				
	60–100	1.18 ± 0.04	0.9 ± 0.5	55	49	4	47	58	5.1	4.5	4.3				
HF3	0–20	1.21 ± 0.09	0.6 ± 0.3	54	30	11	59	75	5.1	4.2	4.5	0.90	10.2	0.08	0.86
	20–40	1.18 ± 0.03	0.4 ± 0.1	55	29	9	62	68	5.2	4.2	4.2				
	40–60	1.12 ± 0.07	0.7 ± 0.1	58	37	8	55	67	5.0	4.3	3.6				
	60–100	1.14 ± 0.02	0.7 ± 0.2	57	39	5	56	66	4.8	4.3	3.3				

[a]Soil classification according to the World Reference Base for Soil Resources (IUSS Working Group WRB, 2022).
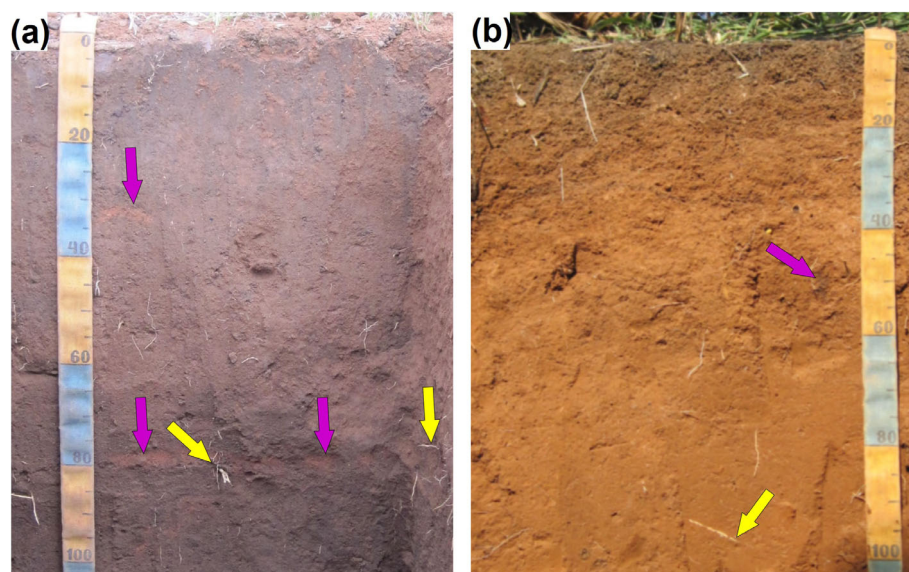[b]Rock fragments (≥2 mm) separated with 2 mm sieve.
[c]Estimated according to soil bulk density.
[d]Potential Cation Exchange Capacity determined with 1 M NH$_4$OAc, at pH 7.
[e]Carbon and nitrogen contents in the first 100 cm of soil profile depth. Concentration as a weighted average (w.t) and stock (kg m^{-2}).
[f]± Standard deviation based on three replicants.

FIGURE 3 Soil profiles with the highest quantity of roots and bioturbation features among the studied Profundihumic Ferralsols (a) and Haplic Ferralsols (b). Profundihumic Ferralsol (a) has more roots at the subsurface (60–100 cm of soil depth) than Haplic Ferralsol (b). The yellow arrows indicate examples of roots at 60 to 100 cm of soil depth in both soil profiles. Once the roots have died and decomposed, they leave behind coarse pores. The purple arrows indicate krotovinas, i.e. bioturbation features (animal burrows) filled with soil. Although all Ferralsols have abundant bioturbation features, the studied Profundihumic Ferralsols contain a greater quantity of krotovinas (especially at 60–100 cm of soil depth) than Haplic Ferralsols.

(Figure 4d). At 60-100 cm of profile depth, the average BC content in Profundihumic Ferralsols (9 ± 2% of total carbon) is nearly double that of Haplic Ferralsols (5 ± 1% of total carbon). Large charcoal fragments (≥1 cm diameter) occupied more than 5% of the area of the soil between 50 and 55 cm of Profundihumic Ferralsols. These charcoal fragments were found in lines parallel to the soil surface.

3.4 | Carbon isotope concentrations

$\delta^{13}C$ values of untreated and treated soils are similar in Profundihumic ($-20 \pm 2‰$) and Haplic Ferralsols ($-20 \pm 1‰$) (Figure 4i,j, Table 3). At the top 40 cm of soil depth, Profundihumic Ferralsols have slightly lower $\delta^{13}C$ values (untreated soils) than the Haplic Ferralsol (Figure 4j). However, no difference was observed in $\delta^{13}C$ values at the subsurface below 40 cm of soil depth. In contrast, $\Delta^{14}C$ values are more negative in Profundihumic Ferralsols than in the Haplic Ferralsol for all soil depths (Figure 4e,h, Table 3). There is a decrease in $\Delta^{14}C$ values as a function of soil depth in all soil profiles indicating that the soils received more inputs of modern carbon from plant debris and roots at the surface (0–30 cm soil depth) compared to deep parts of the soil profile below 30 cm of soil profile depth (Figure 4e,h). $\Delta^{14}C$ values in 0–20 cm of soil depth are $-21 \pm 27‰$ and 37‰

for Profundihumic and Haplic Ferralsols, respectively. Positive $\Delta^{14}C$ values at 0–20 cm of soil depth confirmed that modern carbon inputs occur near the soil surface in association with the presence of fresh roots in the soil profiles. The difference in $\Delta^{14}C$ values between Profundihumic and Haplic Ferralsols is more pronounced at the subsurface (40–60 and 60–100 cm soil depth) than in the top 20 cm of soil depth. At the soil depth interval of 60–100 cm, $\Delta^{14}C$ values are substantially more negative in Profundihumic Ferralsols ($-269 \pm 34‰$) than in the Haplic Ferralsol ($-164‰$). The $\Delta^{14}C$ values of the Ferralsols presented here aligned well with the following global mean $\Delta^{14}C$ values of soils from tropical forests: $+7$ and $-250‰$ for surface and subsurface soils, respectively (Shi et al., 2020). $\Delta^{14}C$ values of PF profiles are similar to the lowest $\Delta^{14}C$ values for soils from savanna: -144 and $-439‰$ for surface and subsurface soils, respectively (Shi et al., 2020).

3.5 | Bulk density, total pore space, and water-stable aggregates

Average bulk density for the entire 0–100 cm of soil depth is lower in Profundihumic Ferralsols (1.05 ± 0.08 kg L^{-1}) than in Haplic Ferralsols (1.21 ± 0.05 kg L^{-1}), p-value < 0.001 (Figure 4b, Table 2). Bulk density in Profundihumic Ferralsols is significantly lower
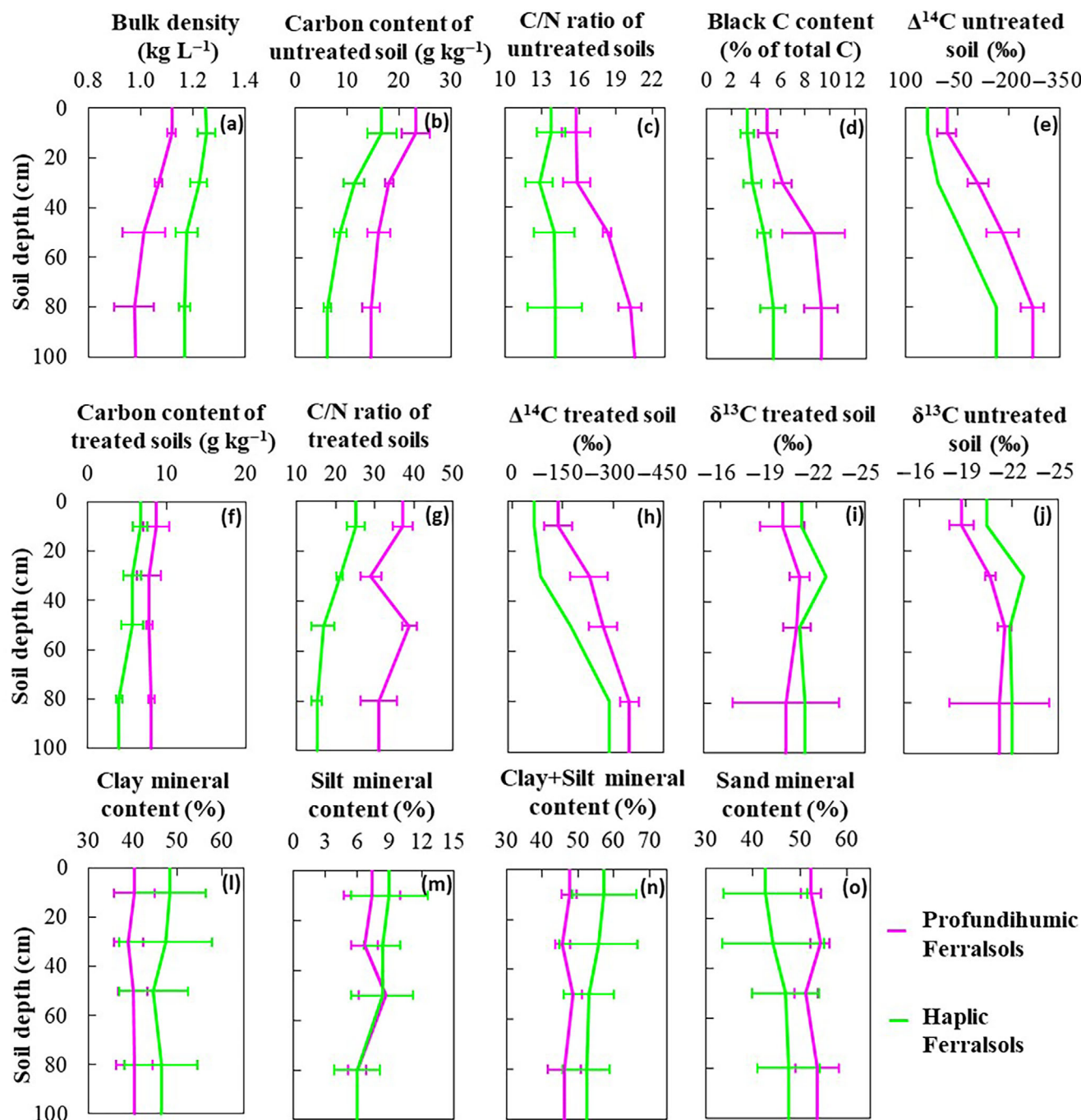
FIGURE 4 Depth profile distribution of the studied soil properties (a): Bulk density of Profundihumic Ferralsols is significantly lower than that of Haplic Ferralsols for all soil depths. (a,b): Bulk density and carbon content of untreated soil follow the same soil depth distribution. (b–e, j): Data of untreated soil (without NaOCl oxidation) indicate that Profundihumic Ferralsols have greater carbon content, C/N ratio, black carbon content, and more negative Δ^{14}C values than Haplic Ferralsols for all soil depths. (c–e): C/N ratio, black carbon content, and Δ^{14}C values have similar soil-depth distribution. (f–i): Data of treated soil with NaOCl oxidation was considered the mineral-associated carbon. Profundihumic and Haplic Ferralsols have a similar mineral-associated carbon content in the first 40 cm of soil depth. (l–o): particle-size distribution does not vary significantly between the studied Ferralsols nor follow the soil-depth distribution of the bulk density. Data from 3 Profundihumic Ferralsols profiles and 3 Haplic Ferralsols profiles (except for Δ^{14}C and δ^{13}C which were determined in 1 Haplic Ferralsols profile and 3 Profundihumic Ferralsols profiles). Horizontal bars correspond to the standard deviations associated to every mean value computed.

than in Haplic Ferralsols for all investigated soil depth intervals, p-value < 0.01 (Figure 4a). The variability of bulk density in the studied Profundihumic Ferralsols is

not a function of the particle size distribution ($r^2 \leq 0.14$) (Data S3, Figure SI3.1–SI3.4). Rather, bulk density and carbon content of soil follow the same soil depth

TABLE 3 Total carbon, nitrogen, black carbon contents, and isotope concentrations in the studied Profundihumic Ferralsols (PF) and Haplic Ferralsols (HF).

| Soil profile/soil class[a]	Depth cm	Untreated samples[c] C g kg^{-1}	N	C/N	δ^{13}C ‰	Δ^{14}C	BC[b] % of total C	Samples treated with NaOCl[d] C g kg^{-1}	N	C/N	δ^{13}C ‰	Δ^{14}C
PF1	0–20	23.4	1.4	17	−18.8	−50.4	5.3	8.1	0.2	41	−19.5	−158.6
	20–40	18.9	1.1	17	−20.4	−103.0	6.3	7.6	0.3	25	−20.8	−197.9
	40–60	19.2	1.0	19	−21.6	−139.0	6.8	7.6	0.2	38	−21.4	−238.5
	60–100	16.9	0.9	19	−23.4	−249.9	9.4	8.1	0.3	27	−22.4	−333.2
PF2	0–20	19.9	1.3	15	−17.8	−27.3	5.7	6.9	0.2	35	−18.3	−174.1
	20–40	18.2	1.1	17	−20.3	−150.2	7.0	5.9	0.2	30	−20.2	−306.5
	40–60	14.5	0.8	18	−21.9	−246.1	12.3	7.4	0.2	37	−21.3	−329.5
	60–100	13.9	0.7	21	−23.5	−316.8	10.9	8.6	0.3	29	−22.4	−388.8
PF3	0–20	26.4	1.8	15	−19.6	15.6	3.9	10.9	0.3	36	−21.7	−79.8
	20–40	17.1	1.2	14	−21.1	−77.2	5.2	9.6	0.3	32	−21.7	−180.9
	40–60	14.4	0.8	18	−20.9	−157.6	7.0	8.3	0.2	42	−19.5	−241.6
	60–100	12.9	0.6	22	−16.6	−239.0	7.6	7.5	0.2	38	−15.4	−323.9
HF1	0–20	20.7	1.6	13	−20.4	37.2	4.0	7.8	0.3	26	−21.1	−67.7
	20–40	14.0	1.1	13	−22.7	6.9	4.0	6.4	0.3	21	−22.6	−83.2
	40–60	10.3	0.8	14	−21.9	−64.1	4.9	3.8	0.3	13	−20.9	−173.9
	60–100	7.1	0.5	14	−22.0	−164.0	6.5	3.4	0.2	17	−21.2	−289.0
HF2	0–20	14.2	0.9	15	na	na	3.0	6.6	0.3	22	na	na
	20–40	9.9	0.7	14	na	na	4.4	6.5	0.3	22	na	na
	40–60	7.6	0.5	16	na	na	5.1	5.9	0.3	20	na	na
	60–100	5.5	0.3	17	na	na	5.7	4.2	0.3	14	na	na
HF3	0–20	15.1	1.2	13	na	na	2.8	5.5	0.2	28	na	na
	20–40	10.0	0.9	11	na	na	2.8	4	0.2	20	na	na
	40–60	8.1	0.7	12	na	na	3.9	7.2	0.4	18	na	na
	60–100	5.8	0.5	11	na	na	4.1	4.3	0.3	14	na	na

Abbreviation: na, data not available.

[a]Soil classification according to the World Reference Base for Soil Resources (IUSS Working Group WRB, 2022).

[b]Black carbon (pyrogenic carbon) determined according to the benzene polycarboxilic acid (BPCA) method (Glaser et al., 1998; Brodowski et al., 2005).

[c]Air-dried soils without NaOCl oxidation.

[d]The residual soil after NaOCl oxidation was considered the mineral-associated carbon (Mikutta et al, 2006).

distribution (Figure 4a,b). When examining soil depth intervals separately, bulk density decreases as a function of the increase in carbon content ($r^2 \geq 0.46$), C/N ratio ($r^2 \geq 0.41$), and black carbon content ($r^2 \geq 0.58$) (Figure 5). However, at the subsurface (60–100 cm soil depth), bulk density has a stronger correlation with carbon content ($r^2 = 0.87$) and black carbon content ($r^2 = 0.71$) compared with the upper 20 cm (Figure 5). Because topsoil (0–20 cm) undergoes more frequent and shorter wetting-drying cycles than the subsurface soil (Silva et al., 2012), we infer that wetting-drying cycles may reduce the effects of organic matter on bulk density near the soil surface compared with the subsurface

(60–100 cm soil depth). Multiple regression models for the entire 0–100 cm of soil depth indicated that bulk density correlated well with carbon content when combined with C/N ratio ($r^2 = 0.51$), black carbon content ($r^2 = 0.75$), and Δ^{14}C ($r^2 = 0.81$) (Figure 6).

Total pore space estimated with bulk density is greater in Profundihumic Ferralsols ($61 \pm 3\%$) than in Haplic Ferralsols ($55 \pm 2\%$). Profundihumic Ferralsols have more water-stable aggregate ($80 \pm 6\%$ of total soil mass) than Haplic Ferralsols ($70 \pm 7\%$ of total soil mass) (Table 2). The amount of water-stable aggregates increases as a function of carbon content in untreated soil ($r^2 = 0.68$) (Data S3, Figure SI3.6).
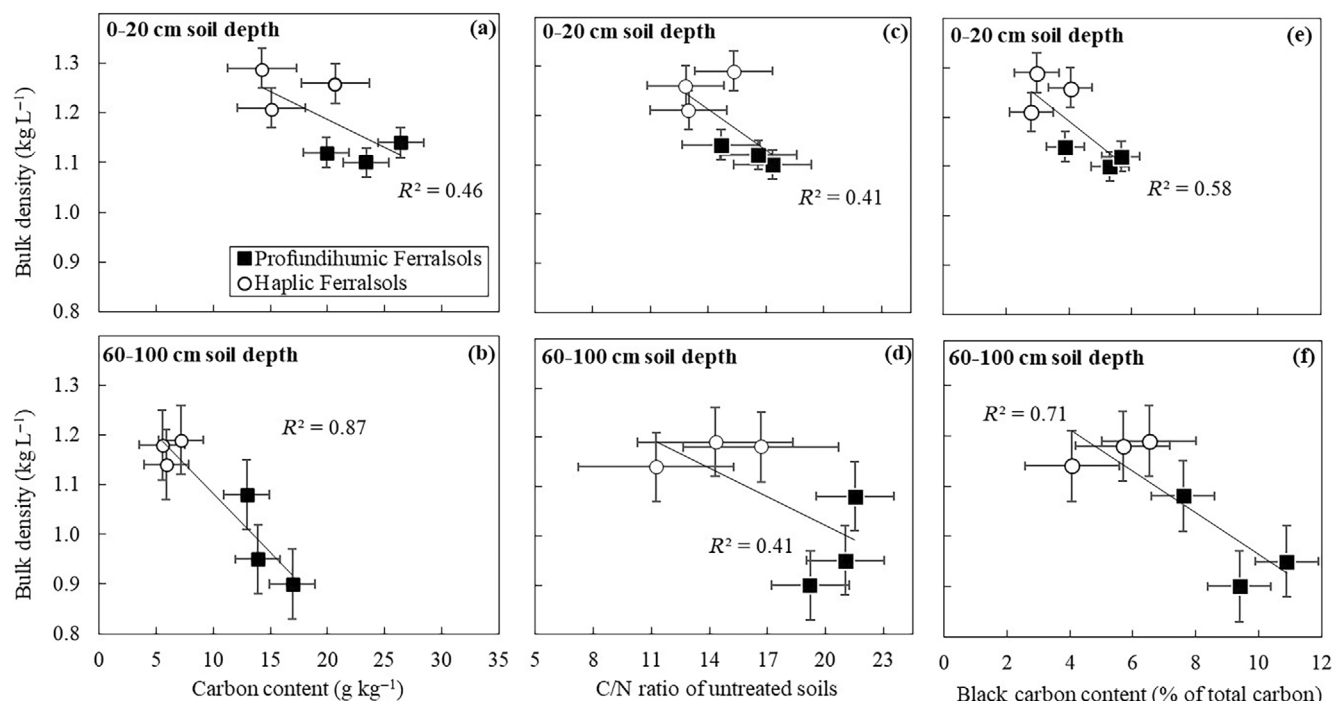
FIGURE 5 Bulk density decreases as a function of carbon content (a/b), C/N ratio (c/d), and black carbon content (e/f) of untreated soils. (a/b): The relationship between bulk density and carbon content is greater at the subsurface (60–100 cm of soil depth) than in the top 20 cm of soil depth. Topsoil (0–20 cm) of Ferralsols undergoes more frequent and short wetting-drying cycles than the subsurface (60–100 cm), thus wetting-drying cycles near the soil surface are likely important players that reduce the effect of organic matter on bulk density. (e/f): Bulk density has a greater correlation to black carbon content at the subsurface than in the topsoil, which is likely associated with a nearly double black carbon content at 60–100 cm soil depth than in the top 20 cm of soil depth. Horizontal and vertical bars correspond to the standard deviations associated to every mean value computed.

3.6 | X-ray computed tomography of soil pores

X-ray computed tomography revealed that total pore volume inside 24 soil aggregates of 4-5 mm diameter does not vary significantly between Profundihumic and Haplic Ferralsols (Figure 7a, Table 4, p-value> 0.4). For this reason, differences in total pore volume between Profundihumic Ferralsols and Haplic Ferralsols are likely caused by processes that influence macroporosity, for example, rooting and borrowing. Disconnected pore volume is greater in Haplic than in Profundihumic Ferralsols (Figure 7b). Pore connectivity is correlated with the carbon content of soils without NaOCl treatment ($r^2 = 0.33$) and with NaOCl-treatment ($r^2 = 0.21$) (Figure 7c,d). For all investigated soils, intra-aggregate pore volume is significantly greater at the subsurface (60–100 cm of soil depth) than in the upper 20 cm of soil depth (Figure 7a, Table 3). Such difference in pore volume is recognizable in the images of soil aggregates from 0 to 20 cm (Figure 7e,f) and 60–100 cm of soil depth (Figure 7g,h).

3.7 | Dilution of the soil particle density by organic matter addition

Although a dilution effect must be considered an obvious physical reality (Adams, 1973; Ruehlmann & Körschens, 2009), our estimated scenarios indicate that a 13-fold increase in carbon content would be required to bring Haplic Ferralsols to the same bulk density level as in Profundihumic Ferralsols (Data S1, Figure SI1.1b).

4 | DISCUSSION

Our results allowed us to reject the hypothesis that bulk density in Profundihumic Ferralsols is a function of particle-size distribution (% of sand, silt, and clay) (Data S3, Figure SI3.1–SI3.4). In addition, the mineralogical composition of Profundihumic Ferralsols is not significantly different from that of all other Ferralsols (Araujo et al., 2017; Marques et al., 2011; Schaefer et al., 2008). Both Profundihumic and Haplic Ferralsols formed from siliciclastic rocks in southeastern Brazil
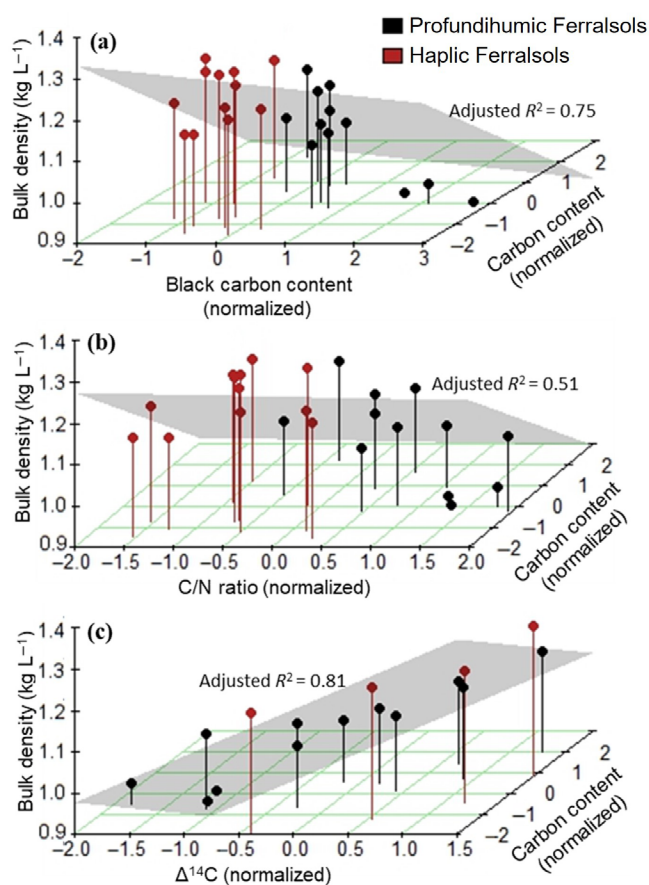
FIGURE 6 Multiples linear regression represented in 3D plots showing that bulk density is a function of carbon content when combined with normalized black carbon content (a), C/N ratio (b), and $\Delta^{14}C$ (c). Soil samples are from the first 100 cm of soil depth. Data of predictor variables were normalized using z-score standardization in the "scale" function in RStudio software.

have essentially a kaolinitic clay mineralogy with lower oxide content compared to Ferralsols from basaltic parent material (Marques et al., 2011; Schaefer et al., 2008). Therefore, we excluded mineral properties as the cause of the low bulk density (high porosity) in the investigated Profundihumic Ferralsols. Rather, the variability in bulk density (and total pore volume) between the studied Ferralsols correlates to carbon content and organic matter composition (C/N ratio and BC content). Based on our models (Data S2) and considering that Profundihumic Ferralsols have just two times more carbon content than all other Ferralsols (Batjes, 1996), we reject the hypothesis that bulk density of Profundihumic Ferralsols was modified by simple dilution of the particle mineral density. We further discuss that it is more likely that organic matter indirectly modifies the porosity (and bulk density) of Profundihumic Ferralsols by stimulating natural bioturbation processes (e.g., rooting and burrowing).

4.1 | Organic matter accumulation increases bioturbation

Bioturbation, also known as the physical displacement of soil materials by organisms, is a key process that influences ecosystem functioning via soil formation (Cosarinsky & Roces, 2007; Johnson et al., 2005; Wilkinson et al., 2009). Bioturbation is also involved in soil aggregation which increases soil porosity and leads to feedback between abiotic and biotic soil components in both the present day and geologic past (Jouquet et al., 2006; Lavelle et al., 2020; Martinez et al., 2019, 2021). Our data emphasize that Profundihumic Ferralsols contain more bioturbation features (roots and burrows) than Haplic Ferralsols in the first 1 m of the soil profile (Figure 3, Table 1). The living roots and decomposing organic matter provide food for the macrofauna that increases porosity in the soil. In our study soils, pores are probably formed by a combination of the three macrofauna actors (termites, ants, and earthworms), although ants and termites are more frequently observed than earthworms in Ferralsols from Brazilian Cerrados (Balbino et al., 2022). Increasing soil organic matter content likely enhances the resources for biological activity of roots and soil animals which would lead to more bioturbation activity, thus, increasing soil porosity. Many studies indicate that root growth increases following the addition of organic matter into the soil (Hoffland et al., 2020; Johnston et al., 2009; Sangakkara et al., 2006). The reason for such a positive relationship is that decayed organic matter supplies nutrients (e.g., nitrogen and phosphorus) that are crucial for plant development (Hoffland et al., 2020; Van der Ploeg et al., 1999). Soil organic matter can also increase water infiltration which benefits the growth of deep roots (Johnston et al., 2009; Sparling et al., 2006). Field and laboratory experiments demonstrate that soil animals (e.g., earthworms) preferentially burrow in soil layers that are rich in organic matter avoiding layers with low organic matter content (Capowiez et al., 2021; Cook & Linden, 1996). Organic matter found as litter at the soil surface or in different forms within the soil profile is food for soil animals and, as such, has a strong influence on their abundance and the intensity of burrowing (Capowiez et al., 2021). Thus, having more organic matter content in Profundihumic Ferralsols than in other Ferralsols would also result in a greater resource for animals and plants in Profundihumic Ferralsols as we observed in the field more roots and animal burrows than in Haplic Ferralsols. However, differential organismic activity could have other reasons than elevated organic matter content, such as soil moisture, particle size distribution, and land use (Johnson et al., 2005; Wilkinson et al., 2009). Soil moisture may be affected by a variety of
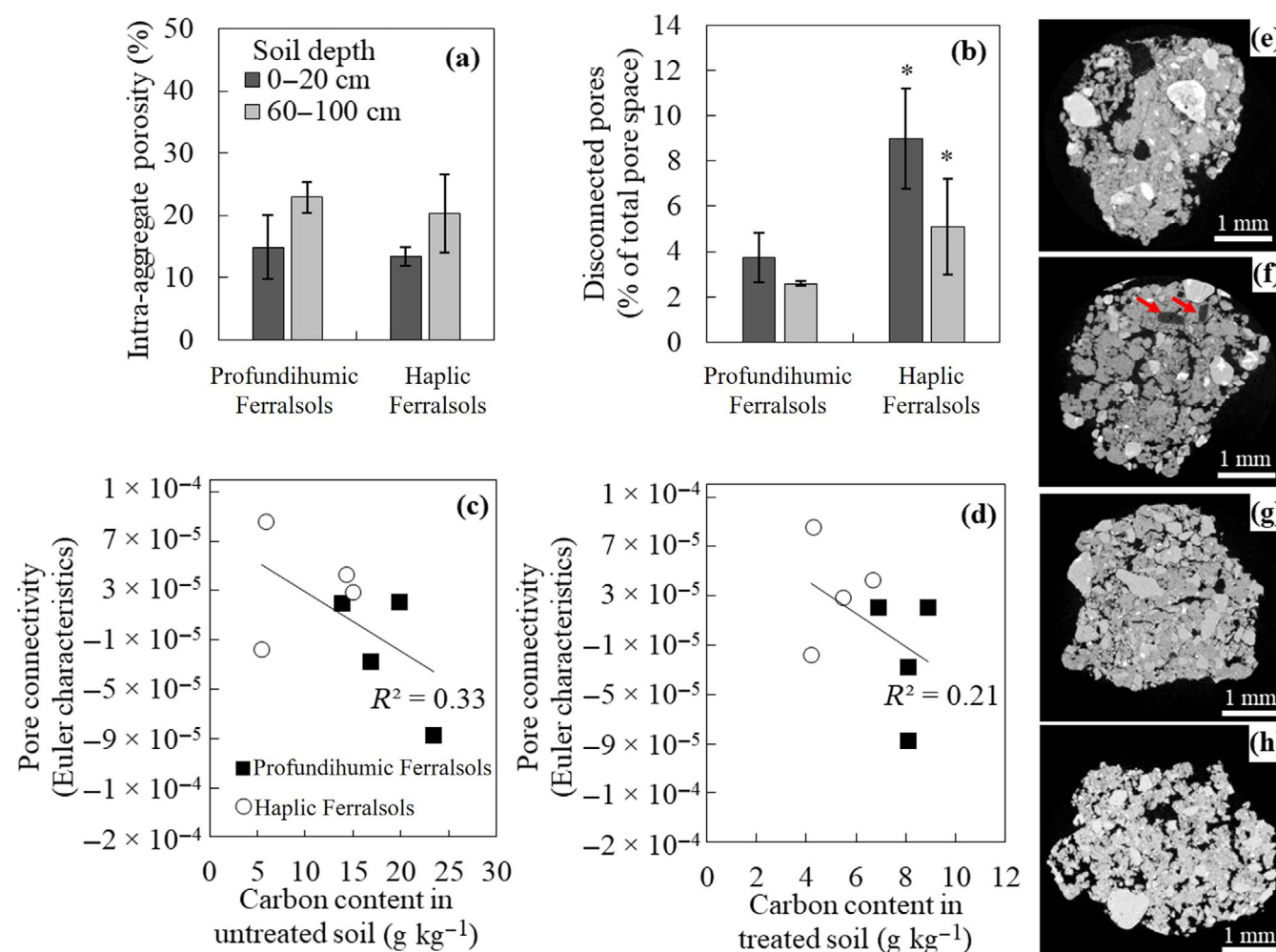
FIGURE 7 Porosity data obtained from X-ray computed tomography of soil aggregates of 4–5 mm diameter. (a) Total pore space inside the aggregates does not significantly differ between Profundihumic Ferralsols and Haplic Ferralsols, p-value >0.4. (b) Disconnected pore space (i.e. investigated pores without connection to the surface of the aggregate) is greater in Haplic than in Profundihumic Ferralsols. The asterisk symbol indicates a significant difference (p-value <0.07). (c/d): Pore connectivity is a function of carbon content in untreated soil (c) in NaOCl-treated samples (d). Euler characteristic is an indicator of pore connectivity. (e–h): Examples of binary images used in this investigation. (e/f): Soil aggregates of Profundihumic Ferralsols from topsoil (0–20 cm depth, e) and subsurface (60–100 cm of soil depth, f). Red arrows indicate small pieces of charcoal. (g/h): Soil aggregates of Haplic Ferralsols from topsoil (0–20 cm depth, e) and 60–100 cm of soil depth (h).

TABLE 4 Porosity parameters determined with X-ray computed tomography of soil aggregates[a] from Profundihumic Ferralsols (PF) and Haplic Ferralsols (HF).

Soil profile	Depth cm	Intra-aggregate pore space %	Disconnected pores[b] % of total pore space
PF1	0–20	19.1 ± 4.2	2.7 ± 1.1
	60–100	24.4 ± 2.1	2.5 ± 0.2
PF2	0–20	10.6 ± 0.6	4.8 ± 1.0
	60–100	21.4 ± 2.0	2.7 ± 0.4
HF2	0–20	15.3 ± 1.4	8.8 ± 1.1
	60–100	20.4 ± 6.2	4.4 ± 2.5
HF3	0–20	11.5 ± 3.3	9.2 ± 3.4
	60–100	20.3 ± 6.3	5.4 ± 2.3

[a]Three soil aggregates of 4–5 mm diameter were analysed per soil depth interval.
[b]Disconnected pores: investigated pores without connection to the surface of the aggregate.
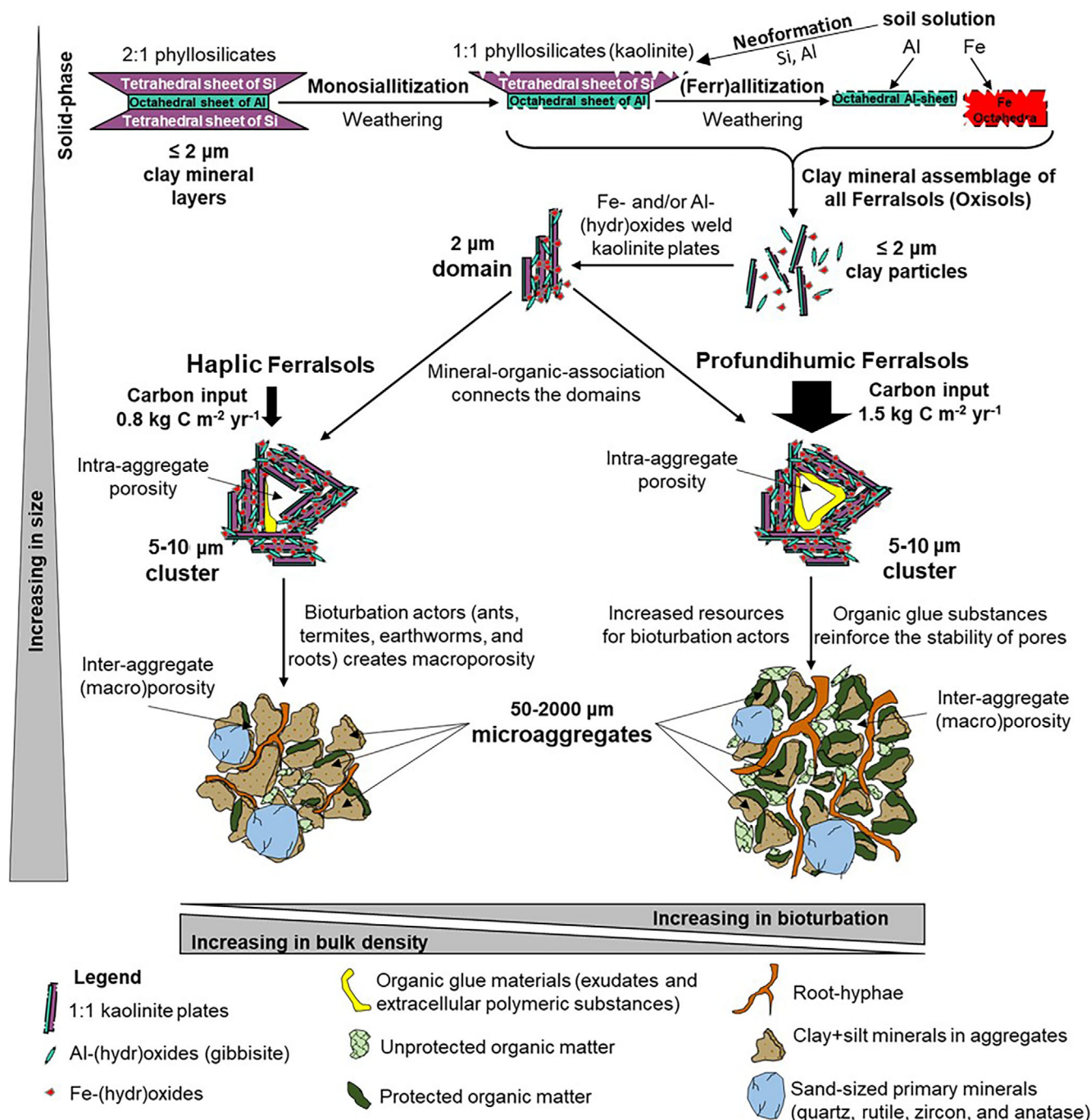
FIGURE 8 Model of pore space formation in Ferralsols as a function of organic matter inputs and bioturbation intensity. The top schematic diagrams show the dissolution of Si tetrahedral sheets in clay minerals and the formation of kaolinite and Al- and/or Fe-(hydr) oxides which are the dominant clay mineral assemblage of Ferralsols. Increasing organic matter input does not increase intra-aggregate porosity (micropores). The high organic matter input augments the resources (energy, nutrients, carbon, and sorption) to bioturbation actors (macrofauna/roots) that drive processes (burrowing, rooting, and production of glue substances) responsible for greater macroporosity and soil aggregate stability in the studied Profundihumic than in Haplic Ferralsols.

soil characteristics (e.g., particle size distribution and porosity) and landscape features (e.g., curvature of the terrain, flooding events, and hydrological regimes upstream). In this study, particle size distribution and land use are constant in both Profundihumic Ferralsols and Haplic Ferralsols. In addition, all soil profiles investigated here are on flat plateaus that are unlikely to receive upstream water flux.

Another piece of evidence for the greater bioturbation activity in Profundihumic Ferralsols than in Haplic

Ferralsols is the abundance of charcoal and BC content ($\sim$10% of total carbon) in deep parts (30–100 cm of soil depth) of Profundihumic Ferralsols profiles. The assumption for how these large charcoal fragments ended up at 50–55 cm of soil depth is that they were buried by soil mesofauna (e.g., termites, ants, and earthworms) who transport soil materials from belowground to the surface and vice-versa, resulting in a "conveyor belt" transport (Darwin, 1881; Johnson et al., 2005; Johnson & Schaetzl, 2015). In southeastern Brazil, such conveyor belt transport of soil materials by soil macrofauna yielded about 0.23 mm yr^{-1} of soil accumulation in the last 8 thousand years (Boulet et al., 1995). Considering such accumulation rates (Boulet et al., 1995), the charcoal fragments would be found at 50 cm of soil depth after nearly 2170 years of soil macrofauna activity. The radiocarbon age of these charcoal fragments is 2030 $\pm$ 20 years BP which corroborated the assumption that these charcoal fragments were once at previous surfaces that were eventually buried by soil macrofauna. However, the occurrence of charcoal fragments and high content of BC content at depth in Profundihumic Ferralsols could be a result of geomorphic processes and/or different fire regime compared to the areas of Haplic Ferralsols. Since all studied Ferralsols here (Profundihumic and Haplic) are formed on correlated stable geomorphic surfaces, we are confident that the Ferralsols selected for our study have been unaffected by modern erosion-deposition processes.

The wider C/N ratio (18–22) in Profundihumic Ferralsols compared to Haplic Ferralsols (11–17) can be taken as evidence of organisms moving relatively undecomposed organic matter (rich in N) from the soil surface to the subsurface. However, the comparatively wide C/N ratio in Profundihumic Ferralsols may also be a side effect of BC enrichment which contains little N. The lower mean values for C/N may also be attributed to the abundant microbial necromass in the soil organic matter found in the subsurface soils compared to plant tissues (Schellekens et al., 2023).

Our findings allowed us to formulate a comprehensive model that explains the differences in porosity and bulk density between Ferralsols with contrasting organic matter accumulation, that is, Profundihumic Ferralsols versus Haplic Ferralsols (Figure 8). Ferralsols formed under intense and extended periods of weathering and leaching, and these processes are determinants for the geochemical transformations of clay minerals: (1) monosiallitization, that is, partial removal of H$_4$SiO$_4$ and formation of 1:1 clay phyllosilicates (kaolinite); and (2) (ferr)allitization, that is desilication and residual accumulation of pedogenic Fe- and/or Al-(hydr)oxides (Buol & Eswaran, 1999) (Figure 8). At the initial stage of

microaggregate formation in Ferralsols, the domains of kaolinite plates are welded by nano-sized Fe- and/or Al-(hydr)oxides into clusters of 5–10 μm which exhibit edge-to-face and edge-to-edge arrangement as well as card-house-type morphology (Bartoli et al., 1992; Vrdoljak & Sposito, 2002) (Figure 8). This arrangement of kaolinite plates and Fe- and/or Al-(hydr)oxides is a determining factor for the formation of highly porous microaggregates in Ferralsols (Buol & Eswaran, 1999; Martinez & Souza, 2020; Oliveira et al., 2005). We found that increasing organic matter input in Profundihumic Ferralsols does not necessarily increase intra-aggregate porosity (microporosity). The involvement of organic matter in the intra-aggregate microporosity is likely predominantly due to extracellular polymeric substances and exudates capable of permeating through small voids (20–50 μm). We posit that the high organic matter inputs likely augment the resources (e.g., nutrients, food source, and moisture) to bioturbation actors who ultimately drive processes (e.g., burrowing, rooting, and production of glue substances) that increase the macroporosity and soil aggregate stability of Profundihumic Ferralsols compared with that of Haplic Ferralsols.

Aligned with the concept of bio-tillage (i.e. the use of plant roots as a tillage tool to manipulate soil structure and porosity to obtain conditions beneficial for crop growth; Zhang & Peng, 2021), we highlight that improvements in the porosity of highly weathered soils exposed to compaction may be attained by land management practices that stimulate the natural bioturbation processes of roots and soil macrofauna. Although the stimulation of bioturbation activity can indeed be used to improve key ecological functions (water availability to plants or producing fertility hot-spots), there are serious issues when bioturbation actors (e.g., termites and ants) attack crops and constructions (Jouquet et al., 2018, 2020). Further studies on how bioturbators (termites, ants, and earthworms) affect soil porosity may take the organic matter inputs in Profundihumic Ferralsols as benchmarks, including a high organic matter input ($\sim$1.5 kg C m^{-2} year^{-1}) bearing a well-balanced C/N ratio (20–25) and BC content that represents $\sim$10% of total carbon.

5 | CONCLUSIONS

Understanding the effects of high organic matter inputs on soil bulk density and related porosity is important for the development of conservation measures in highly weathered soils, including attempts to recover soils exposed to compaction. Based on physical, chemical, and morphological attributes (e.g., bulk density, particle size

distribution, pore characteristics, and nitrogen and carbon content), we determined the direct and indirect effects of organic matter content on soil porosity across different soil depths in Profundihumic and Haplic Ferralsols. Our analysis ruled out particle-size distribution as a potential explanation for the low bulk density (high porosity) of Profundihumic Ferralsols. In addition, a simple dilution of mineral density by increased organic matter input is not the reason for the differences in bulk density between the studied Profundihumic and Haplic Ferralsols. Our results indicate that increased organic matter inputs may enhance the resources (energy, nutrients, carbon, and sorption) for bioturbation actors (plants, earthworms, ants, termites, etc.) that physically rework soil materials through rooting and burrowing, thus increasing porosity and decreasing bulk density. We suggest that soil conservation practices aiming to recover Ferralsols from compaction may be successful if they encourage the bioturbation processes of roots and soil macrofauna. Last, we suggest that the insights obtained from this investigation of Ferralsols should be tested in controlled experiments and for other soil orders of global significance, especially such with deep A-horizons as found in the Chernozems.

AUTHOR CONTRIBUTIONS

Pedro Martinez: Conceptualization; investigation; funding acquisition; writing – original draft; methodology; writing – review and editing. **Rebecca Lybrand:** Writing – review and editing. **Karis J. McFarlane:** Methodology; formal analysis; writing – review and editing; investigation; data curation; funding acquisition. **Maoz Dor:** Investigation; methodology; visualization; writing – review and editing. **Adrian C. Gallo:** Formal analysis. **Amy Mayedo:** Formal analysis. **Fillipe Marini:** Visualization. **Pablo Vidal-Torrado:** Investigation; funding acquisition; writing – review and editing; validation. **Markus Kleber:** Conceptualization; supervision; investigation; writing – original draft; methodology; writing – review and editing.

ACKNOWLEDGEMENTS

DATA AVAILABILITY STATEMENT

ORCID

Pedro Martinez https://orcid.org/0000-0002-6219-4344

REFERENCES

Adams, W. A. (1973). The effect of organic matter on the bulk and true densities of some uncultivated podzolic soils. *Journal of Soil Science*, *24*, 10–17.

Alvares, C. A., Stape, J. L., Sentelhas, P. C., Gonçalves, J. L. M., & Sparovek, G. (2013). Köppen's climate classification map for Brazil. *Meteorologische Zeitschrift*, *22*, 711–728.

Amelung, W., Brodowski, S., Sandhage-Hofmann, A., & Bol, R. (2008). Combining biomarker with stable isotope analyses for assessing the transformation and turnover of soil organic matter. *Advances in Agronomy*, *100*, 155–250.

Araujo, J. K. S., de Souza Júnior, V. S., Marques, F. A., Voroney, P., Souza, R. A. S., Corrêa, M. M., & Câmara, E. R. G. (2017). Umbric Ferralsols along a climosequence from the Atlantic coast to the highlands of northeastern Brazil: Characterization and carbon mineralization. *Geoderma*, *293*, 34–43.

Aviles, A. M. C., Ricardi-Branco, F., Ledru, M. P., & Bernacci, L. C. (2019). Vegetation and climate changes in the forest of Campinas, São Paulo state, Brazil, during the last 25,000 cal yr BP. *Brazilian Journal of Geology*, *49*, e20190040.

Balbino, L. C., Bruand, A., Brossard, M., Grimaldi, M., Hajnos, M., & Guimarães, M. D. F. (2022). Changes in porosity and microaggregation in clayey Ferralsols of the Brazilian Cerrado on clearing for pasture. *European Journal of Soil Science*, *53*, 219–230.

Bartoli, F., Philippy, R., & Burlin, G. (1992). Influence of organic matter on aggregation in Oxisols rich in gibbsite or in goethite. I. Structures: The fractal approach. *Geoderma*, *54*, 231–257.

Batista, E. M., Shultz, J., Matos, T. T., Fornari, M. R., Ferreira, T. M., Szpoganicz, B., Freitas, R. A., & Mangrich, A. S. (2018). Effect of surface and porosity of biochar on water holding capacity aiming indirectly at preservation of the Amazon biome. *Scientific Reports*, *8*, 1–9.

Batjes, N. H. (1996). Total carbon and nitrogen in the soils of the world. *European Journal of Soil Science*, *47*, 151–163.

Boulet, R., Pessenda, L. C. R., Telles, E. C. C., & Melfi, A. J. (1995). Evaluation of the rate of surface biological accumulation of soil matter using radiocarbon dating on charcoal and soil humin fraction. A Case Study of Oxisols from the Basin of the Lagoa Campestre, Salitre, Minas Gerais, Brazil. *Comptes Rendus de l'Académie Des Sciences Numérisés sur le site de la Bibliothèque Nationale de France*, *320*, 287–294.

Broek, T. A., Ognibene, T. J., McFarlane, K. J., Moreland, K. C., Brown, T. A., & Bench, G. (2021). Conversion of the

LLNL/CAMS 1 MV biomedical AMS system to a semi-automated natural abundance 14C spectrometer: System optimization and performance evaluation. *Nuclear Instruments and Methods in Physics Research Section B: Beam Interactions with Materials and Atoms*, 499, 124–132. https://doi.org/10.1016/j.nimb.2021.01.022

Bruand, A., Cousin, I., Nicoullaud, B., Duval, O., & Begon, J. C. (1996). Backscattered electron scanning images of soil porosity for analyzing soil compaction around roots. *Soil Science Society of America Journal*, 60, 895–901.

Bruand, A., & Reatto, A. (2022). Morphology, chemical composition and origin of 2: 1 phyllosilicates in Bw horizons of latosols of the Brazilian central plateau: Contribution to the discussion of the microgranular structure origin. *Comptes Rendus Géoscience*, 354, 159–185.

Bruand, A., Reatto, A., & Souza Martins, É. (2022). Allochthonous material originating from saprolite as a marker of termite activity in Ferralsols. *Scientific Reports*, 12, 17193.

Buol, S. W., & Eswaran, H. (1999). Oxisols. *Advances in Agronomy*, 68, 151–195.

Calegari, M. R. (2008). Ocorrência e significado paleoambiental do Horizonte A húmico em Latossolos. Ph.D. Thesis, University of São Paulo. https://doi.org/10.11606/T.11.2009.tde-11032009-093135

Capowiez, Y., Gilbert, F., Vallat, A., Poggiale, J. C., & Bonzom, J. M. (2021). Depth distribution of soil organic matter and burrowing activity of earthworms—Mesocosm study using X-ray tomography and luminophores. *Biology and Fertility of Soils*, 57, 337–346.

Cook, S. M., & Linden, D. R. (1996). Effect of food type and placement on earthworm (Aporrectodea tuberculata) burrowing and soil turnover. *Biology and Fertility of Soils*, 21, 201–206.

Cosarinsky, M. I., & Roces, F. (2007). Neighbor leaf-cutting ants and mound-building termites: Comparative nest micromorphology. *Geoderma*, 141, 224–234.

Curtis, R. O., & Post, B. W. (1964). Estimating bulk density from organic-matter content in some Vermont forest soils. *Soil Science Society of America Journal*, 28, 285–286.

Darwin, C. (1881). *The formation of vegetable Mould, through the action of Worms, with observations on their habits*. J. Murray.

De Vos, B., Van Meirvenne, M., Quataert, P., Deckers, J., & Muys, B. (2005). Predictive quality of pedotransfer functions for estimating bulk density of forest soils. *Soil Science Society of America Journal*, 69, 500–510.

Farmer, V. C. (1982). Significance of the presence of allophane and imogolite in podzol Bs horizons for podzolization mechanisms: A review. *Soil Science and Plant Nutrition*, 28, 571–578.

Ferreira, I. C. D. M., Coelho, R. M., Torres, R. B., & Bernacci, L. C. (2007). Soil and native vegetation remnant in Campinas, SP, Brazil. *Pesquisa Agropecuária Brasileira*, 42, 1319–1327.

Glaser, B., Haumaier, L., Guggenberger, G., & Zech, W. (1998). Black carbon in soils: The use of benzenecarboxylic acids as specific markers. *Organic Geochemistry*, 29, 811–819.

Gugino, B. K., Idowu, O. J., Schindelbeck, R. R., van Es, H. M., Wolfe, D. W., Moebius-Clune, B. N., Thies, J. E., & Abawi, G. S. (2009). Cornell Soil Health Assessment Training Manual, Edition 2.0, Cornell University, Geneva, NY.

Hoffland, E., Kuyper, T. W., Comans, R. N., & Creamer, R. E. (2020). Eco-functionality of organic matter in soils. *Plant and Soil*, 455, 1–22.

IPT-Instituto de Pesquisas Tecnológicas do Estado de São Paulo. (1981). Mapa Geológico do Estado de São Paulo, escala 1: 500.000.

IUSS Working Group WRB. (2022). World Reference Base for Soil Resources. International soil classification system for naming soils and creating legends for soil maps. 4th edition. International Union of Soil Sciences (IUSS), Vienna, Austria.

Johnson, D. L., Domier, J. E. J., & Johnson, D. N. (2005). Animating the biodynamics of soil thickness using process vector analysis: A dynamic denudation approach to soil formation. *Geomorphology*, 67, 23–46.

Johnson, D. L., & Schaetzl, R. J. (2015). Differing views of soil and pedogenesis by two masters: Darwin and Dokuchaev. *Geoderma*, 237, 176–189.

Johnston, A. E., Poulton, P. R., & Coleman, K. (2009). Soil organic matter: Its importance in sustainable agriculture and carbon dioxide fluxes. *Advances in Agronomy*, 101, 1–57.

Jouquet, P., Chaudhary, E., & Kumar, A. R. V. (2018). Sustainable use of termite activity in agro-ecosystems with reference to earthworms: A review. *Agronomy for Sustainable Development*, 38, 1–11.

Jouquet, P., Dauber, J., Lagerlöf, J., Lavelle, P., & Lepage, M. (2006). Soil invertebrates as ecosystem engineers: Intended and accidental effects on soil and feedback loops. *Applied Soil Ecology*, 32, 153–164.

Jouquet, P., Traoré, S., Harit, A., Choosai, C., Cheik, S., & Bottinelli, N. (2020). Moving beyond the distinction between the bright and dark sides of termites to achieve sustainable development goals. *Current Opinion in Insect Science*, 40, 71–76.

Kleber, M., & Jahn, R. (2007). Andosols and soils with andic properties in the German soil taxonomy. *Journal of Plant Nutrition and Soil Science*, 170, 317–328.

Kleber, M., Mikutta, R., Torn, M. S., & Jahn, R. (2005). Poorly crystalline mineral phases protect organic matter in acid subsoil horizons. *European Journal of Soil Science*, 56, 717–725.

Lavelle, P., Spain, A., Fonte, S., Bedano, J. C., Blanchart, E., Galindo, V., Grimaldi, M., Jimenez, J. J., Velasquez, E., & Zangerlé, A. (2020). Soil aggregation, ecosystem engineers and the C cycle. *Acta Oecologica*, 105, e103561.

Lehmann, J., Rillig, M. C., Thies, J., Masiello, C. A., Hockaday, W. C., & Crowley, D. (2011). Biochar effects on soil biota–a review. *Soil Biology and Biochemistry*, 43, 1812–1836.

Marques, F. A., Buurman, P., Schellekens, J., & Vidal-Torrado, P. (2015). Molecular chemistry in humic Ferralsols from Brazilian Cerrado and forest biomes indicates a major contribution from black carbon in the subsoil. *Journal of Analytical and Applied Pyrolysis*, 113, 518–528.

Marques, F. A., Calegari, M. R., Vidal-Torrado, P., & Buurman, P. (2011). Relationship between soil oxidizable carbon and physical, chemical and mineralogical properties of umbric ferralsols. *Revista Brasileira de Ciência Do Solo*, 35, 25–40.

Martinez, P., Buurman, P., do Nascimento, D. L., Almquist, V., & Vidal-Torrado, P. (2021). Substantial changes in podzol morphology after tree-roots modify soil porosity and hydrology in a tropical coastal rainforest. *Plant and Soil*, 463, 77–95.

Martinez, P., Buurman, P., Lopes-Mazzetto, J. M., Nascimento, D. L., & Vidal-Torrado, P. (2019). Podzolisation preserves ichnofossils constructed by ghost shrimp. *Catena*, 180, 110–119.

Martinez, P., Silva, L. C. R., Calegari, M. R., Camargo, P. B., Vidal-Torrado, P., & Kleber, M. (2022). Carbon stocks in umbric ferralsols driven by plant productivity and geomorphic processes, not by mineral protection. *Earth Surface Processes and Landforms*, *47*, 491–508.

Martinez, P., & Souza, I. F. (2020). Genesis of pseudo-sand structure in Oxisols from Brazil–a review. *Geoderma Regional*, *22*, e00292.

Neufeldt, H., Resck, D. V. S., Ayarza, M. A., & Zech, W. (1999). Soil organic matter in oxisols of the Brazilian Cerrados. In R. Thomas & M. A. Ayarza (Eds.), *Sustainable land Management for the Oxisols of the Latin American savannas* (pp. 89–107). CIAT (Centro Internacional de Agricultura Tropical), Cali.

Oliveira, T. S., de Costa, L. M., & Schaefer, C. E. (2005). Water-dispersible clay after wetting and drying cycles in four Brazilian oxisols. *Soil and Tillage Research*, *83*, 260–269.

Pessoa, T. N., Cooper, M., Nunes, M. R., Uteau, D., Peth, S., Vaz, C. M. P., & Libardi, P. L. (2022). 2D and 3D techniques to assess the structure and porosity of Oxisols and their correlations with other soil properties. Catena, 210:e.105899.

Pribyl, D. W. (2010). A critical review of the conventional SOC to SOM conversion factor. *Geoderma*, *156*, 75–83.

Reatto, A., Bruand, A., de Souza Martins, E., Muller, F., da Silva, E. M., de Carvalho Jr, O. A., Brossard, M., & Richard, G. (2009). Development and origin of the microgranular structure in latosols of the Brazilian central plateau: Significance of texture, mineralogy, and biological activity. *Catena*, *76*, 122–134.

Regelink, I. C., Stoof, C. R., Rousseva, S., Weng, L., Lair, G. J., Kram, P., Nikolaidis, N. P., Kercheva, M., Banwart, S., & Comans, R. N. (2015). Linkages between aggregate formation, porosity and soil chemical properties. *Geoderma*, *247*, 24–37.

Ross, J. L. S., & Moroz, I. C. (1996). Mapa geomorfológico do estado de São Paulo. *Revista Do Departamento de Geografia*, *10*, 41–58.

Ruehlmann, J., & Körschens, M. (2009). Calculating the effect of soil organic matter concentration on soil bulk density. *Soil Science Society of America Journal.*, *73*, 876–885.

Sangakkara, U. R., Pietsch, G., Gollner, M., & Freyer, B. (2006). Impact of organic matter and method of addition on selected soil parameters, growth and yields of mungbean grown in a minor season in the humid tropics. *Die Bodenkultur: Journal of Land Management, Food and Environment*, *57*, 25–31.

Schaefer, C. E. (2001). Brazilian latosols and their B horizon microstructure as long-term biotic constructs. *Soil Research*, *39*, 909–926.

Schaefer, C. E. G. R., Fabris, J. D., & Ker, J. C. (2008). Minerals in the clay fraction of Brazilian latosols (Oxisols): A review. *Clay Minerals*, *43*, 137–154.

Schellekens, J., Justi, M., Macedo, R., Calegari, M. R., Buurman, P., Kuyper, T. W., Barbosa de Camargo, P., & Vidal-Torrado, P. (2023). Long-term carbon storage in Brazilian Cerrado soils–a conjunction of wildfires, bioturbation, and local edaphic controls on vegetation. *Plant and Soil*, *484*, 645–662.

Schmidt, M. W., Torn, M. S., Abiven, S., Dittmar, T., Guggenberger, G., Janssens, I. A., Kleber, M., Kögel-Knabner, I., Lehmann, J., Manning, D. A., & Nannipieri, P. (2011). Persistence of soil organic matter as an ecosystem property. *Nature*, *478*, 49–56.

Schoeneberger, P. J., Wysocki, D. A., & Benham, E. C. (2012). Field book for describing and sampling soils, Version 3.0. Natural Resources Conservation Service, National Soil Survey Center, Lincoln.

Shi, Z., Allison, S. D., He, Y., Levine, P. A., Hoyt, A. M., Beem-Miller, J., Zhu, Q., Wieder, W. R., Trumbore, S., & Randerson, J. T. (2020). The age distribution of global soil carbon inferred from radiocarbon measurements. *Nature Geoscience*, *13*, 555–559.

Silva, S. G. C., Silva, Á. P. D., Giarola, N. F. B., Tormena, C. A., & Sá, J. C. D. M. (2012). Temporary effect of chiseling on the compaction of a Rhodic hapludox under no-tillage. *Revista Brasileira de Ciência Do Solo*, *36*, 547–555.

Siregar, A., Kleber, M., Mikutta, R., & Jahn, R. (2005). Sodium hypochlorite oxidation reduces soil organic matter concentrations without affecting inorganic soil constituents. *European Journal of Soil Science*, *56*, 481–490.

Sparling, G. P., Wheeler, D., Vesely, E. T., & Schipper, L. A. (2006). What is soil organic matter worth? *Journal of Environmental Quality*, *35*, 548–557.

Stuiver, M., & Polach, H. A. (1977). Discussion reporting of 14C data. *Radiocarbon*, *19*, 355–363.

Swanson, A. C., Schwendenmann, L., Allen, M. F., Aronson, E. L., Artavia-León, A., Dierick, D., Fernandez-Bou, A. S., Harmon, T. C., Murillo-Cruz, C., Oberbauer, S. F., & Pinto-Tomás, A. A. (2019). Welcome to the Atta world: A framework for understanding the effects of leaf-cutter ants on ecosystem functions. *Functional Ecology*, *33*, 1386–1399.

Torn, M. S., Swanston, C. W., Castanha, C., & Trumbore, S. E. (2009). Storage and turnover of organic matter in soil. In *Biophysico-chemical processes involving natural nonliving organic matter in environmental systems* (pp. 219–272). John Wiley & Sons, Inc.

Tranter, G., Minasny, B., McBratney, A. B., Murphy, B., McKenzie, N. J., Grundy, M., & Brough, D. (2007). Building and testing conceptual and empirical models for predicting soil bulk density. *Soil Use and Management*, *23*, 437–443.

Van der Ploeg, R. R., Böhm, W., & Kirkham, M. B. (1999). On the origin of the theory of mineral nutrition of plants and the law of the minimum. *Soil Science Society of America Journal*, *63*, 1055–1062.

Velasco-Molina, M., Berns, A. E., Macías, F., & Knicker, H. (2016). Biochemically altered charcoal residues as an important source of soil organic matter in subsoils of fire-affected subtropical regions. *Geoderma*, *262*, 62–70.

Villela, F. N. J., Sanches Ross, J. L., & Manfredini, S. (2013). Relief-rock-soil relationship in the transition of Atlantic plateau to peripheral depression, Sao Paulo, Brazil. *Journal of Maps*, *9*(3), 343–352.

Vogel, H. J., Balseiro-Romero, M., Kravchenko, A., Otten, W., Pot, V., Schlüter, S., Weller, U., & Baveye, P. C. (2022). A holistic perspective on soil architecture is needed as a key to soil functions. *European Journal of Soil Science*, *73*, e13152.

Volland-Tuduri, N., Bruand, A., Brossard, M., Balbino, L. C., de Oliveira, M. I. L., & de Souza Martins, É. (2005). Mass proportion of microaggregates and bulk density in a Brazilian clayey Oxisol. *Soil Science Society of America Journal*, *69*, 1559–1564.

Vrdoljak, G., & Sposito, G. (2002). Soil aggregate hierarchy in a Brazilian Oxisol. *Developments in Soil Science*, *28*, 197–217.

Wildenschild, D., & Sheppard, A. P. (2013). X-ray imaging and analysis techniques for quantifying pore-scale structure and

processes in subsurface porous medium systems. *Advances in Water Resources*, *51*, 217–246.

Wilkinson, M. T., Richards, P. J., & Humphreys, G. S. (2009). Breaking ground: Pedological, geological, and ecological implications of soil bioturbation. *Earth-Science Reviews*, *97*, 257–272.

Xiong, P., Zhang, Z., & Peng, X. (2022). Root and root-derived bio-pore interactions in soils: A review. *Journal of Plant Nutrition and Soil Science*, *185*, 643–655.

Zhang, Z., Dong, X., Wang, S., & Pu, X. (2020). Benefits of organic manure combined with biochar amendments to cotton root growth and yield under continuous cropping systems in Xinjiang, China. *Scientific Reports*, *10*, 1–10.

Zhang, Z., & Peng, X. (2021). Bio-tillage: A new perspective for sustainable agriculture. *Soil and Tillage Research*, *206*, 104844.

SUPPORTING INFORMATION

Additional supporting information can be found online in the Supporting Information section at the end of this article.